JOC The Journal of Organic Chemistry

ARTICLE

pubs.acs.org/joc

Ring-Expanded Bicyclic β-Lactams: A Structure−Chiroptical Properties Relationship Investigation by Experiment and Calculations

Magdalena Woźnica,[†] Aleksandra Butkiewicz,[†] Aneta Grzywacz,[†] Patrycja Kowalska,[†] Marek Masnyk,[†] Karol Michalak,[†] Roman Luboradzki,[‡] Filipp Furche,*[,§] Holger Kruse,[⊥] Stefan Grimme,*[,⊥] and Jadwiga Frelek*[,†]

[†]Institute of Organic Chemistry of the Polish Academy of Sciences, Kasprzaka 44, 01-224 Warsaw, Poland

[‡]Institute of Physical Chemistry of the Polish Academy of Sciences, Kasprzaka 44, 01-224 Warsaw, Poland

[§]Department of Chemistry, University of California, Irvine, Natural Sciences II, Irvine, California 92697-2025, United States

[⊥]Organisch-Chemisches Institut der Universität Münster, Corrensstrasse 40, 48149 Münster, Germany

Supporting Information

ABSTRACT: In the present work, the validity of the helicity rule relating the absolute configuration of the bridgehead carbon atom in bicyclic β-lactams to the sign of the 220 nm band observed in their electronic circular dichroism (ECD) spectra is examined for ring-expanded cephalosporin analogues. To this end, a series of model compounds with a seven-membered ring condensed with the β-lactam unit was synthesized. A key step of their synthesis was either the ring-closing metathesis (RCM) or the free radical cyclization leading to the seven-membered ring with an S, O, or C atom at the 6 position in the bicyclic skeleton. To investigate the scope and limitations of the simple, empirically established helicity rule, a combination of ECD spectroscopy, variable-temperature ECD measurements, X-ray analysis, and time-dependent density functional theory (TD-DFT) calculations was used. A comparison of the experimental ECD spectra with the spectra simulated by TD-DFT calculations gives a reasonable interpretation of the Cotton effects observed in the 240−215 nm spectral range. The results suggest that the helicity rule does not apply to the investigated compounds because of the planarity of their amide chromophore. Thus, these compounds do not constitute an exception to the rule that was established for bi- and polycyclic β-lactams with the nonplanar amide chromophore only.

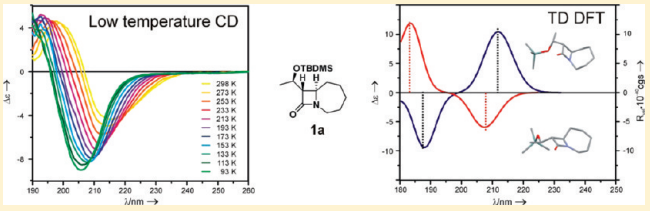

1. INTRODUCTION

The β-lactam family of antibiotics represents one of the most clinically relevant families of antibiotics known.[1] This is attributable to their broad spectrum of antibacterial activity and a relatively low level of toxicity.[2] It has also been proved that only β-lactam antibiotics with an *R* absolute configuration at the ring junction carbon atom display strong antibacterial activity.[3] Therefore, the relationship between an *R* absolute configuration at the bridgehead carbon atom and the sign of the lowest energy Cotton effect (CE) attributed to the amide n → π* transition, which occurs in penicillins and cephalosporins at around 230 and 260 nm, respectively, was extensively investigated.[3a,c,4] Frelek at al. contributed to the studies on this subject with investigation of chiroptical properties of 5-dethia-5-oxacephams.[5] As a result, a simple helicity rule was proposed that permits the assignment of absolute configuration at the ring junction carbon atom based on the sign of the ECD band at around 220 nm arising from the amide n → π* excitation. It was also found that the same rule is valid for clavams,[6] cephams,[7] carbacephams,[7] natural penicillins, and cephalosphorins and their saturated and unsaturated derivatives as well.[8] Very recently, we demonstrated the successful applicability of the rule to carbapenams.[9]

On the basis of X-ray analysis and computational studies, it was demonstrated that the most important feature of the molecular structure shared by all compounds examined so far is the nonplanarity of amide chromophoric system.[5,6b,6c,7,8] This nonplanarity of the chromophore causes its intrinsic dissymmetry and is expressed in a right- or left-handed helicity depending upon the absolute configuration at the bridgehead carbon atom. Thus, on the basis of the helicity rule we were able to correlate the *R* absolute configuration at the ring junction with a positive sign of the Cotton effect (CE) attributed to the amide n → π* transition and the *S* absolute configuration with a negative sign of the same CE.

To validate the helicity rule established under the assumption of conformational rigidity of the bicyclic system and the realization that most of the molecular excitations are localized within the amide chromophore, we conducted a detailed theoretical study.[7] As the method of choice we applied the time-dependent density functional theory (TD-DFT) as it has become an important tool in theoretical CD spectroscopy due to a reasonable balance between accuracy and computational efficiency.[10] The results of our study revealed a high sensitivity of the ECD spectra to the configuration at the bridgehead carbon atom and a surprisingly high sensitivity to the molecular conformation and substitution of the five- or six-membered rings.[7,8] The molecular

Received: January 28, 2011
Published: March 25, 2011

dynamics (MD) simulations carried out for carbacephams revealed a considerable flexibility of the saturated six-membered ring and a high dependency of the ECD spectra on the conformation of both the four- and the six-membered rings. In some cases, this dependency resulted in the sign inversions for both n → π* and π → π* bands at various points of the MD simulation. Thus, in some oxacephams a breakdown of the helicity rule occurred, likely caused by a change of the conformation of the pyranose ring from a chair to a boat.[7] Therefore, the question arose about the scope and limitations of the helicity rule. To answer this question several model compounds with a β-lactam ring fused to the seven-membered ring were synthesized (Chart 1). These compounds were selected as models because of their greater conformational flexibility in comparison with the investigated bicyclic β-lactams with the five- or six-membered rings condensed with an azetidinone ring. Therefore, a different set of CEs for different conformations present in the equilibrium can be expected for these compounds. Moreover, a flattening of the amide chromophore can occur in β-lactams **1**−**10**, due to the lower strain energy of the seven-membered ring. For this reason, a noncompliance with the helicity rule is conceivable because the rule was developed for the skewed bi- and polycyclic β-lactams only.

To get more insight in the structure−ECD spectra relationship, we will apply a combined treatment of experimental ECD spectroscopy and TD-DFT. Furthermore, we will address the question about the effect of Boltzmann averaging the theoretical spectra of several conformers and corresponding theoretical requirements on computed conformational energies. Since ECD spectroscopy is very sensitive to smallest changes in the geometry and electronic structure of the investigated molecules, the combination of experimental and theoretical ECD results should allow us to draw more definite conclusions within the scope of present research. This combination has already proven efficient and reliable for the assignment of the absolute configuration of various chiral organic molecules.[11]

Chart 1

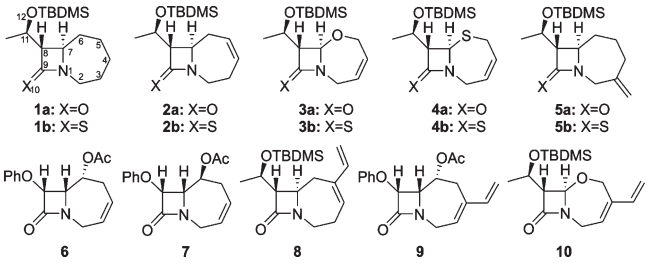

2. RESULTS AND DISCUSSION

2.1. Synthesis. Compounds **1a**, **2a**, **3a**, and **4a** were synthesized according to Scheme 1 in which the key step is the ring-closing metathesis (RCM) of 1,8-nonanadiene system leading to a seven-membered ring.

As a starting material in this synthesis the commercially available azetidinone **11** was used. In the first step the acetoxy group was substituted in the reaction with allyl bromide, allyl alcohol, or allyl thioalcohol, yielding compounds **12a**, **12b**, and **12c**, respectively. Compound **12a** was subjected to alkylation reaction with 4-bromo-1-butene in the presence of sodium hydride, and compounds **12b** and **12c** were reacted analogously with 1-bromo-3-propene. Resulting compounds **13a**−**13c** were ready for RCM, which was performed in boiling methylene chloride in the presence of catalytic amounts of Grubbs' first-generation catalyst, providing compounds **2a**, **3a**, or **4a**. The double bond in compound **2a** was then hydrogenated with H_2 over palladium on charcoal to yield **1a**.

Compound **5a** was prepared according to Scheme 2. In the first step compound **12a** was alkylated at the nitrogen atom with 2,3-dibromo-1-propene giving product **14**, which was converted into **5a** in the free radical cyclization reaction with tributyltin hydride in the presence of catalytic amounts of AIBN.

Compounds **6** and **7** were also obtained using the RCM of 1,8-nonanadiene system; however, readily obtainable compound **15** was used as the starting material (Scheme 3).[12] As a first step,

Scheme 2[a]

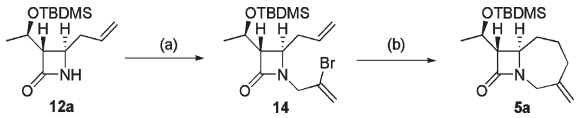

[a] Legend: (a) 2,3-dibromopropene, NaH, DMF, rt; (b) AIBN, Bu_3SnH, C_6H_6, 80 °C.

Scheme 1[a]

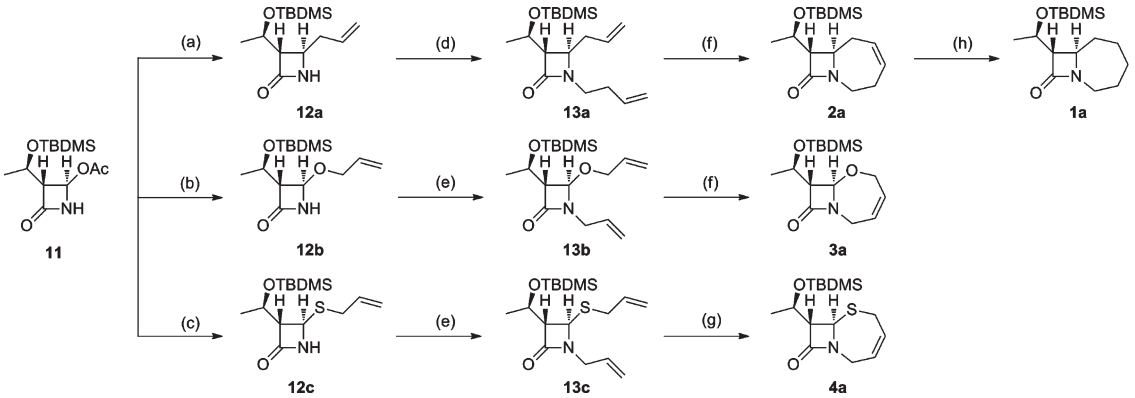

[a] Legend: (a) allyl bromide, KI, In, DMF, rt; (b) allyl alcohol, $Pd(OAc)_2$, Et_3N, C_6H_6, rt; (c) allyl thioalcohol, BuLi, THF, −78 °C, rt; (d) 4-bromo-1-butene, NaH, rt; (e) allyl bromide, NaH, DMF, rt; (f) Grubbs' I cat. (5 mol%), CH_2Cl_2, 40 °C; (g) Grubbs' I cat. (20 mol %), CH_2Cl_2, 40 °C; (h) H_2, Pd/C, EtOH, rt.

dx.doi.org/10.1021/jo200171w |J. Org. Chem. 2011, 76, 3306–3319

Scheme 3[a]

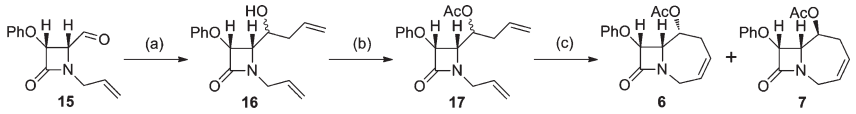

[a] Legend: (a) allyl bromide, Zn, NH_4Cl(sat.), THF, 0 °C, rt; (b) Ac_2O, Py; (c) Hoveyda−Grubbs' II cat. (10 mol %).

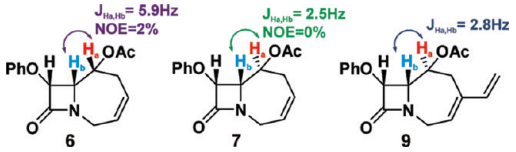

Figure 1. ^{1}H difference NOE experiments of compounds **6** and **7** and diagnostic coupling constants for **9**.

the aldehyde **15** was transformed into a chromatographically nonseparable mixture of alcohols **16**. The alcohols were acetylated with acetic anhydride, and acetates **17** were subjected to RCM reaction yielding a mixture of **6** and **7** in the ratio of 1: 1.

A sample of the mixture of **6** and **7** was separated into pure diastereomers using HPLC technique. The absolute configuration at C6 carbon atom was assigned using NOE experiment, as shown in Figure 1.

Compound **8** was prepared using an enyne variant of metathesis according to Scheme 4. First, the acetoxy group in azetidinone **11** was substituted by the propargyl chain in the reaction with propargyl bromide and indium in the presence of potassium iodide.[13] The alkylation product **18** was then alkylated at nitrogen atom with 4-bromo-1-butene under the PTC condition with pulverized potassium hydroxide, yielding enyne **19**, which was subjected to RCM using Hoveyda−Grubbs' second-generation catalyst (Hoveyda−Grubbs' II). As a result the bicyclic product **8** was formed.

Compound **9** was prepared according to Scheme 5 starting from aldehyde **15**, which was reacted with propargyl bromide and zinc to produce alcohol **20**. Acetylation of alcohol **20** followed by the metathesis reaction with Hoveyda−Grubbs' second-generation catalyst provided bicyclic product **9**. Interestingly, compound **9** was the only diastereomer obtained in this reaction. The indicated absolute configuration at C6 carbon atom was determined by comparing the appropriate coupling constants in the ^{1}H NMR spectra of compounds **6**, **7**, and **9** as shown in Figure 1.

Compound **10** was prepared according to Scheme 6 starting from azetidinone **11**. The acetoxy group was replaced by propargyl ether leading to compound **22**. Alkylation of **22** at the nitrogen atom with allyl bromide and sodium hydride as a base gave product **23**, which was converted into the bicyclic system **10** in the metathesis reaction with Grubbs' first-generation catalyst (Grubbs' I).

The thiono analogous **1b**, **2b**, **3b**, **4b**, and **5b** were obtained by direct thionation of **1a**, **2a**, **3a**, **4a**, and **5a** in the reaction with Lawesson's reagent.[14]

2.2. Experimental ECD Results. The ECD and UV data are collected in Table 1. On the basis of the presented data compounds **1**−**10** can be classified by *R* or *S* absolute configuration at the ring junction and the presence of an additional chromophore interfering with the amide absorption bands. As evident from Table 1, up to four absorption bands within the spectral range of 185−300 nm are present in the ECD spectra of investigated compounds **1**−**10**. For the purpose of our studies, however, the band occurring between 212 and 238 nm is of a particular interest because this band is the subject of the helicity rule. This band can be attributed to the amide n(O) → π^* transition, and its corresponding electronic UV absorption is hidden by the neighboring absorption bands (see Table 1). In the case of β-lactams **1a**−**5a**, the decisive ECD band occurs at about 215 nm, whereas in the case of **6**−**10** its position is shifted to the lower energy region by around 10−15 nm. This is likely related to the presence of an interfering diene chromophore that absorbs in a similar energy range as the amide chromophore.

To follow the helicity rule, the sign of the decisive ECD band should be positive for β-lactams belonging to the 7*R*-configurational series, that is, compounds **1**−**5**, **8**, and **10**, whereas it should be negative for β-lactams **6**, **7**, and **9**, representing the 7*S*-configurational series. In fact, in the ECD spectra of β-lactams with the 7*R*-configuration a negative sign of the CE at around 215 nm is present and a positive one of the same CE for β-lactams with 7*S*-configuration (Table 1, Figure 2). This result contradicts the prediction made by the helicity rule and, in fact, calls for the assessment of the validity of the rule for this class of compounds. It is therefore necessary to examine whether compounds **1**−**10** are the exception to the rule or, more generally, the rule itself is imperfect.

The origin of the inconsistency between the experimental results and predictions made applying the rule is undoubtedly very important for further studies on similar systems. Conformational flexibility of the investigated systems and/or a planarity of the chromophore might explain these unexpected results. The planarity of the chromophore will prevent the use of the helicity rule because the rule was developed for β-lactams with a nonplanar amide chromophore only.[5,8] Conformational flexibility of the seven-membered ring may also lead to a sign change as different conformers can make different contributions to the total ensemble-averaged spectrum.

To find reasons for possible breakdown of the helicity rule, the TD-DFT calculations and variable low-temperature ECD measurements were carried out for selected β-lactams. The results should give more insight into the conformational and chiroptical behavior of compounds **1**−**10**.

2.3. Theoretical ECD Results and Variable Low-Temperature ECD Measurements. To confirm and assign the experimental and computational ECD spectra, first the thermally accessible conformational species of the respective molecule must be obtained. For this prerequisite the MMX force field from the PCModel 9.1[15] software was used. The structures thus obtained were subsequently reoptimized at the dispersion corrected[16] BLYP-D[17]/def2-TZVP[18] level of theory. For all conformers found within a 3 kcal/mol energy window, more accurate B2PLYP-D[19]/def2-QZVP[18] single point calculations were performed to obtain a reliable Boltzmann distribution. The COSMO solvation model[20] was used to simulate the effects of the solvent (acetonitrile; dielectric constant of ε = 36.64) and was included in all TD-DFT calculations.

All TD-DFT calculations were carried out with the TURBOMOLE suite of programs.[21] For BLYP-D the resolution of

dx.doi.org/10.1021/jo200171w |*J. Org. Chem.* 2011, 76, 3306–3319

Scheme 4[a]

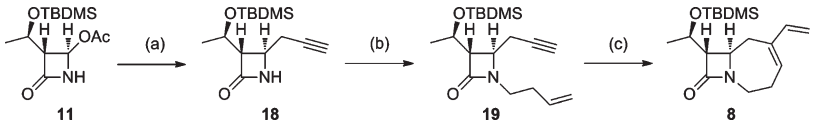

[a] Legend: (a) propargyl bromide, KI, In, DMF, rt; (b) 4-bromo-1-butene, PTC conditions; (c) Hoveyda−Grubbs' II cat. (10 mol%), CH_2Cl_2, 40 °C.

Scheme 5[a]

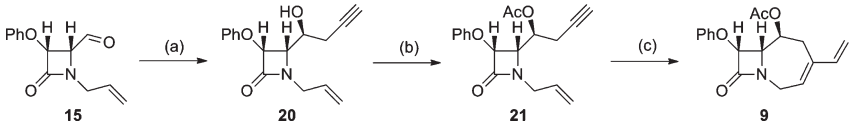

[a] Legend: (a) propargyl bromide, Zn, NH_4Cl (sat), THF, 0 °C; (b) Ac_2O, Py, rt; Hoveyda−Grubbs' II cat. (10 mol %), CH_2Cl_2, 40 °C.

Scheme 6[a]

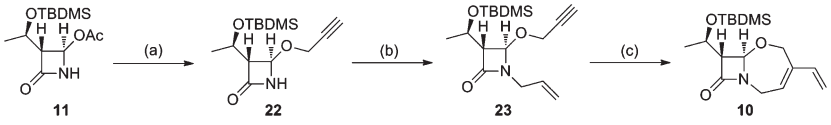

[a] Legend: (a) propargyl alcohol, $Zn(OAc)_2$, toluene, 80 °C; (b) allyl bromide, NaH, DMF, rt; (c) Grubbs' I cat. (10 mol %), CH_2Cl_2, 40 °C.

Table 1. UV and ECD Data of β-Lactams 1−10 Recorded in Acetonitrile in the Range of 186−300 nm

compd	UV ε (λ_{max}); [M^{-1} cm^{-1} (nm)]			CD $\Delta\varepsilon$ (λ_{max}); [M^{-1} cm^{-1} (nm)]			
1a				+2.4 (199.0)		−3.6 (216.0)	+0.7 (238.0)
2a	920 (196)			+4.9 (193.0)		−9.3 (211.5)	+0.2 (234.0)
3a			500 (237^{sh})	+9.4 (187.5)		−12.1 (214.0)	
4a			520 (244^{sh})	+33.0 (189.0)	−7.3 (205.5)	−11.2 (220.5)	+1.3 (248.5)
5a					+9.2 (201.5)	−7.0 (219.5)	
6	32000 (192)	6500 (218^{sh})	800 (269)	−2.4 (187.0)	+10.1 (202.0)	+2.5 (228.5)	−0.2 (266.0)[a]
7	44500 (192)	9900 (218^{sh})	1200 (268)	−9.9 (187.5)	+25.1 (202.0)	+3.5 (229.5)	−0.2 (265.0)[a]
8	13000 (196)		13700 (234)	−10.3 (197.0)	+2.0 (212.5)	−4.8 (238.0)	
9	43800 (192)	19250 (220)	3100 (269)	−8.3 (202.0)[b]	+2.4 (216.5^{sh})	+14.6 (231.0)	−0.5 (268.0)[a]
10		12700 (227)	1100 (276)	+17.5 (192.0)		−10.8 (223.0)	+0.4 (261.5)

[a] An additional small positive ECD band is observed at around 280 nm. [b] An additional negative ECD band is observed at around 188 nm.

identity[22] (RI, density fitting) of the Coulomb integrals has been applied. Likewise, B2PLYP-D makes use of the RI-MP2 code within the ricc2 module.[23] The necessary auxiliary basis sets were taken from the TURBOMOLE library.[20] The convergence criterion for the optimizations regarding the change of total energy between two subsequent optimization cycles was set to 10^{-7} E_h and the numerical quadrature grid of *m4* quality was used throughout.

The vertical excitation energies and rotational strengths in dipole lengths form were calculated with the escf module[24] according to the TD-PBE0 formalisms with the def2-TZVPP[18] basis set. Because a fully consistent COSMO/TD-DFT treatment of electronically excited states is technically not possible at the moment, we applied the COSMO model to the calculation of the ground state and solely used the COSMO modified orbitals and eigenvalues in a subsequent standard gas-phase TD-DFT treatment. All theoretical CD spectra were simulated by overlapping Gaussian functions for each transition. A value of σ = 0.2 eV for the width of the absorption band at a height of 1/e was chosen.

For compound **5a** a modified approach was chosen, which was extensively validated in ref 5, where the reader is referred for further details. The structure was optimized using a split-valence basis set with a set of polarization functions on non-hydrogen atoms [SV(P)].[18] SV(P) energetics were validated with polarized triple-ζ valence basis sets (def2-TZVP).[25] Fine quadrature grids (size m4) were employed.[25b,26] All stationary points were confirmed to be minima by the force-constant calculations. Excitation energies and rotatory strengths of the lowest 20 singlet states were computed using TD-DFT[26] and SV(P) basis sets. CD spectra were simulated by superposition of Gaussians with a uniform line width of 0.16 eV. Solvent effects were taken into account by the COSMO model[21] using the dielectric constant of acetonitrile (37.5). The slightly different dielectric constant used here is neglectable in the COSMO model. The fast response of the screening potential was neglected in the TD-DFT response calculations. The one-parameter hybrid density functional of Perdew, Burke, and Ernzerhof (PBE0)[26] was used throughout.

dx.doi.org/10.1021/jo200171w |*J. Org. Chem.* 2011, 76, 3306–3319

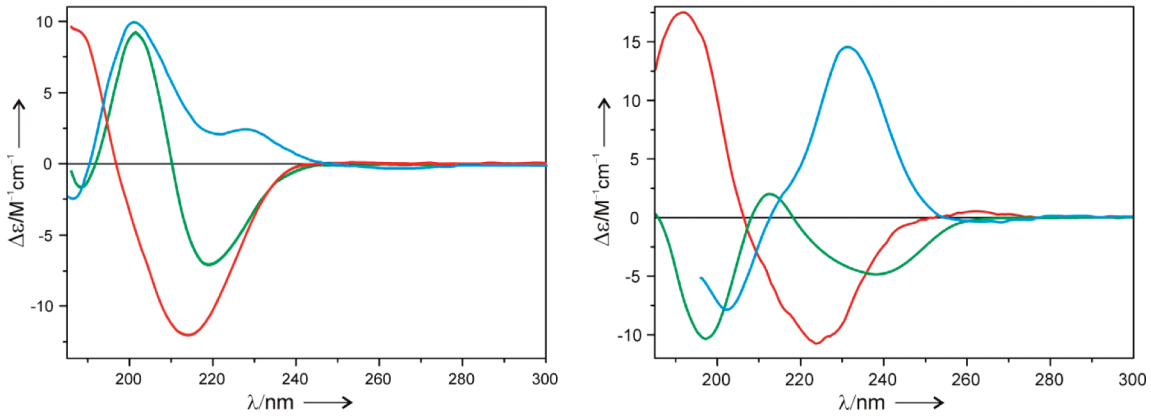

Figure 2. Experimental ECD spectra of β-lactams. Left: **3a** (red line), **6** (blue line), and **5a** (green line). Right: **8** (green line), **9** (blue line), and **10** (red line) recorded in acetonitrile. The symbol ε denotes the molar decadic absorption coefficient and λ the wavelength.

Table 2. Overview of the Conformer Analysis for Compound 1a[a]

conformer	ΔE	population	10-9-1-2	10-9-1-7	8-9-1-2	8-9-1-7	7-8-11-12	pyramid.
1	0.00	49.9	−2.5	+179.8	+178.1	+0.4	−69.1	−1.7
2	0.43	24.1	+0.1	+179.5	−179.6	−0.2	+48.0	−0.5
3	0.75	14.0	−21.1	−177.2	+158.0	+1.9	−69.6	+18.2
4	1.23	6.2	−20.1	−177.3	+158.4	+1.9	+49.3	+17.3
5	1.73	2.7	−3.2	−178.9	+177.0	+1.2	+48.1	+3.2
6	2.25	1.1	−3.0	−178.8	+177.2	+1.4	+179.2	+3.2
7	2.38	0.8	+3.3	−179.3	+176.6	+0.6	−179.2	+2.9

[a] Selected torsion angles in degrees and pyramidal heights (pyramid.) for the N-atom in pm determined on the basis of COSMO-BLYP-D/def-TZVP structures. Pyramidal height defined as a deviation from planarity according to Radhakrishnan et al.[27] Relative energies ΔE (kcal/mol), computed at COSMO-B2LYP-D/def2-QZVP level of theory. Conformer population at 25°C in %.

For β-lactam **1a** seven conformers in the energy range of 2.4 kcal/mol were found. To simplify the calculation, the large substituent at C8 (OSi^tBuMe_2) has been replaced by smaller $OSiMe_3$ group. Both of these groups have very similar electronic properties, and interchanging them does not influence the electronic spectra significantly. Furthermore, the effect on the conformational space is also expected to be small. The calculations were done in a similar fashion for the other compounds. The only exception is β-lactam **5a**, for which the *tert*-butyl group was taken into account.

As can be seen in Table 2, two out of seven conformers obtained for **1a**, namely, 3 and 4, possess slightly skewed amide chromophores, whereas in the remaining five the chromophoric system is planar. The seven-membered ring in conformers of **1a** is in a chair or a twist-chair conformation, and the azetin-2-one ring is in an equatorial position at C7 (Figure 3). Beyond that, the individual conformers show conformational differences mostly in the substituent on C8 carbon atom.

For the negative sign of the O10−C9−N1−C2 and O10−C9−N1−C7 torsion angles, the helicity rule predicts a positive sign of the crucial ECD band. In accordance with this, a positive sign of the lowest energy excitations is calculated for conformers 3 and 4 (Figure 3f and g). The sign of the same band in conformers with a planar amide chromophore, i.e., conformers 1, 2, 5, 6, and 7 (see Table 2), is negative and therefore not subject to the helicity rule. The population ratio of conformers with a planar and nonplanar chromophore in β-lactam **1a** is found to be approximately 4:1. Therefore, in the average ECD spectrum comprising, by definition, the sum of contributions from all populated conformers, the negative sign of the decisive band should predominate, which is indeed the case (Figure 3h). However, a small positive ECD band at around 240 nm, originating from the twisted conformers 3 and 4, is present in both experimental and simulated spectra. The band at around 220 nm has primarily the character of an amide n $\rightarrow \pi^*$ transition. The average ECD spectrum shows very close agreement between experiment and theory, thus providing strong evidence that these conformers are present in solution under these conditions (Figure 3h).

Only two chair conformers have been calculated for β-lactam **5a** in the energy range of 3 kcal/mol. In agreement with the experiment, the simulated ECD spectrum of the lowest energy chair conformer (chair 1) with a planar amide chromophore exhibits a negative sign of the 220 nm CE and therefore does not conform to the helicity rule. The simulated ECD spectrum of the second chair conformer of **5a** (chair 2) displays a positive sign of the same CE in agreement with the helicity rule. The amide chromophore in this conformer is twisted as demonstrated by the torsion angle O10−C9−N1-C2 equal to −12.24°. Since this conformer is computed to be 2.4 kcal/mol (PBE0/def2-TZVP) higher in energy than the lowest energy chair 1 conformer, its population is negligible at room temperature. Therefore, there is apparently no difference between the simulated ECD spectrum of chair 1 conformer and the Boltzmann-averaged spectrum (Figure 4). To fully account for different orientations of the flexible TBDMS side chain and quantitatively predict the ECD spectrum, especially at higher energies, molecular dynamics simulations would be necessary.

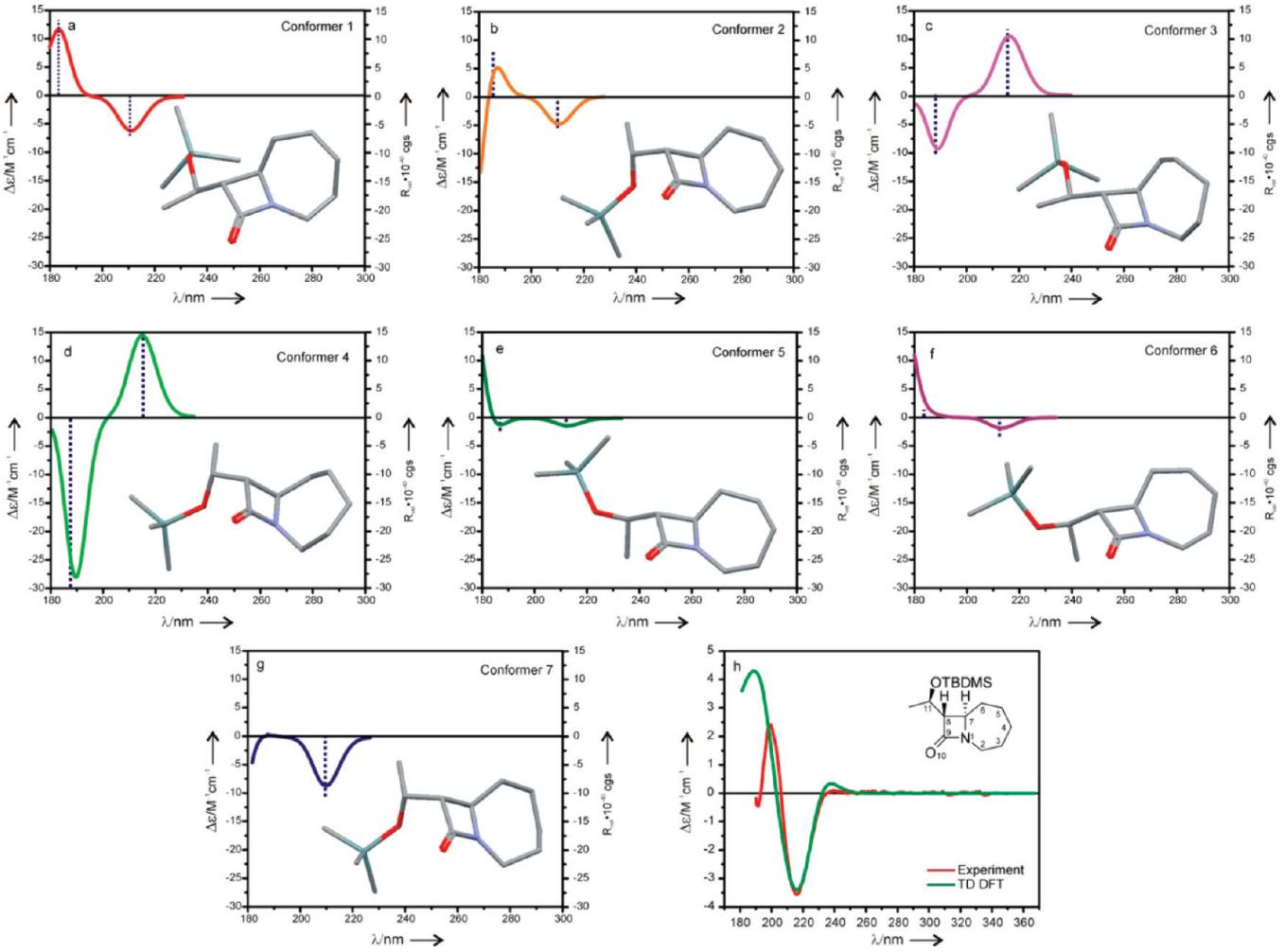

Figure 3. (a−g) COSMO-BLYP-D/def-TZVP structures of conformers of β-lactam **1a** and their computed ECD spectra at the TD-PBE0/def2-TZVPP level of theory. (h) Boltzmann-averaged spectrum compared to experiment. The symbol ε denotes the molar decadic absorption coefficient, λ is the excitation wavelength, and R is the computed rotatory strength.

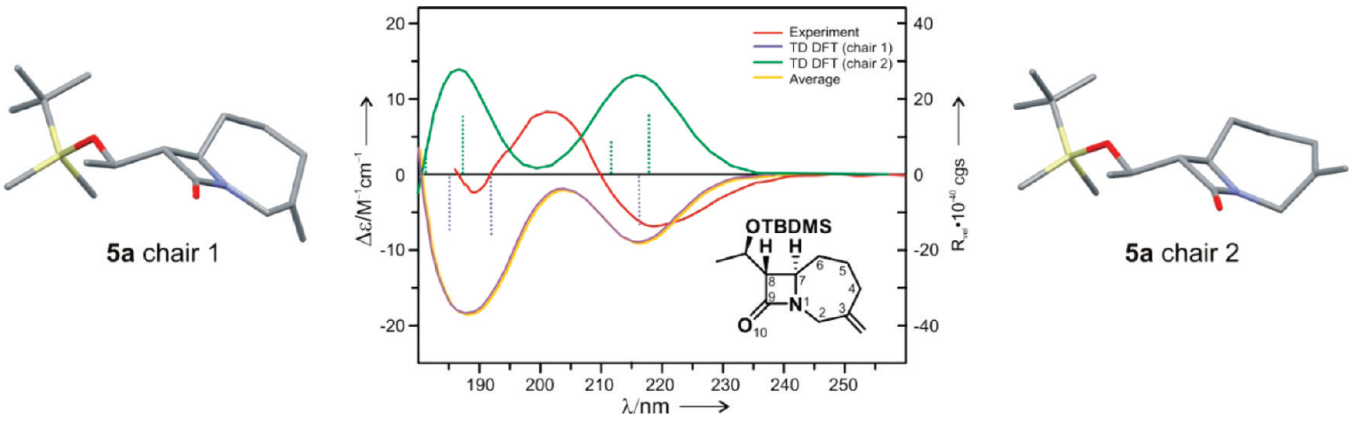

Figure 4. COSMO-PBE0/SV(P) structures of conformers of β-lactam **5a** and their computed ECD spectra at the TD-PBE0/def2-TZVP level of theory together with the Boltzmann-averaged spectrum compared to experiment. The symbol ε denotes the molar decadic absorption coefficient, λ is the excitation wavelength, and R is the computed rotatory strength.

The agreement between the experimental and Boltzmann-averaged ECD spectra is very satisfactory also for β-lactams **2a**−**4a** (Figure 5). In these cases, depending on the compound, the main ECD band is a mixture of excitations out of the amide n → π^* transition and transitions out of the sulfur or oxygen lone pairs into the same acceptor orbitals. In addition, the transitions

dx.doi.org/10.1021/jo200171w |*J. Org. Chem.* 2011, 76, 3306–3319

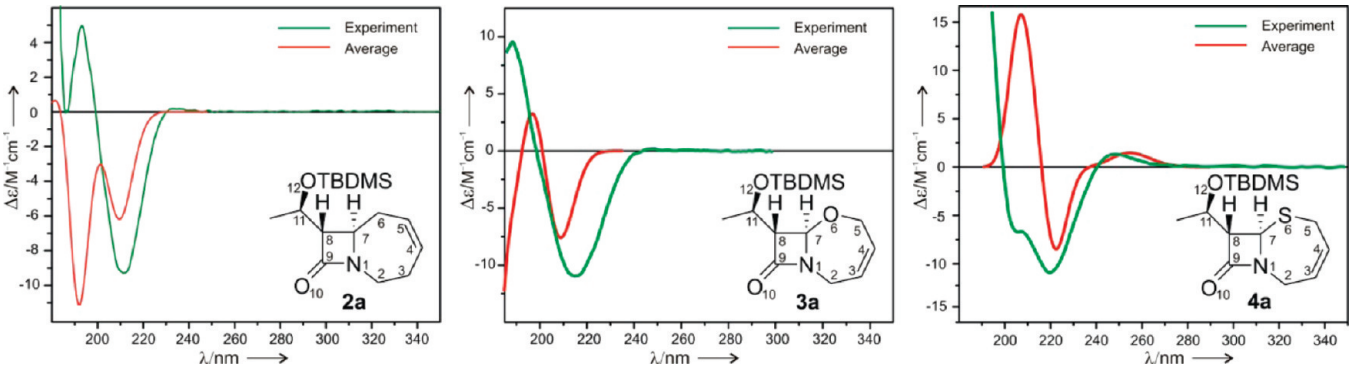

Figure 5. Boltzmann-averaged TD-PBE0/def2-TZVPP spectra compared to experiment of β-lactams **2a**−**4a**. The symbol ε denotes the molar decadic absorption coefficient, and λ is the excitation wavelength.

Table 3. Overview of the Conformer Analysis for Compound 8[a]

conformer	ΔE	population	10-9-1-2	10-9-1-7	8-9-1-2	8-9-1-7	7-8-11-12	pyramid.
1	0.00	72.24	−7.9	−178.5	+172.0	+1.4	−68.6	+6.9
2	0.76	20.15	−6.1	−178.7	+172.4	−0.2	+48.3	+5.4
3	1.66	4.41	−7.1	−179.3	+172.4	+0.2	−88.9	+5.6
4	2.06	2.24	−4.1	−179.2	+174.8	−0.3	+47.0	+3.5
5	3.00	0.46	−16.3	−177.5	+162.8	+1.6	−69.5	+14.4

[a] Selected torsional angles in degrees and pyramidal height (pyramid.) for the N-atom in pm determined on the basis of COSMO-BLYP-D/def-TZVP structures. Relative energies ΔE (kcal/mol) computed at COSMO-B2PLYP-D/def2-QZVP level of theory. Conformer population at 25°C in %.

out of the double bond orbitals mix strongly with the amide n → π^* transition. Some of the structures of conformers of β-lactams **2a**−**4a**, calculated in the range of 3 kcal/mol, demonstrate a small deviation of the amide chromophore from planarity manifested by a slight pyramidality of the amide nitrogen. Nevertheless, the negative sign of the decisive ECD band in both experimental and Boltzmann-averaged ECD spectra clearly demonstrates the breakdown of the helicity rule for these compounds.

A more complex situation occurs in compounds **6**−**10** due to the presence of groups strongly interfering with the amide chromophore. The phenoxy and acetoxy substituents at C8 and C6, respectively, present in β-lactams **6**, **7**, and **9** absorb at similar wavelengths as the amide chromophore, which considerably complicates the ECD spectra. In the case of β-lactams **8**−**10** the additional presence of a highly absorbing and strongly interfering diene system introduces a further complication.

As shown in Table 3, five conformers have been found for β-lactam **8** in the energy range of 3 kcal/mol. Two of them, namely, conformers 1 and 2, constitute more than 90% of the conformational mixture. Thus, these conformers predominate at room temperature. The simulated ECD spectra of both conformers, despite the negative sign of the O10−C9−N1−C2 torsion angle, show a negative sign of the CE at 238 nm (Figure 6). It is worth adding that in the case of **8**, the CE at 238 nm is due mainly to the electronic excitation within the diene system, absorption of which predominates the net ECD spectrum.

Six contributing conformers were found for compound **9** within a 1.6 kcal/mol energy range (see Supporting Information). The two lowest energy conformers, populated with 58% and 24%, respectively, dominate the net ECD spectrum. The O10−C9−N1−C2 torsion angle in **9** is positive, just as is the sign of the CE at 238 nm.

Nevertheless, the positive/negative sign of the ECD band at around 230 nm, decisive in terms of the helicity rule, in the case of compounds studied is in contradiction to the rule because for the *S*/*R* configuration at the bridge-head carbon atom the rule predicts a negative or a positive sign of this band, respectively. To provide further evidence and to find experimental confirmation for the computational results, the variable low-temperature ECD spectra of selected β-lactams were recorded. However, to achieve a better resolution of the ECD bands, the β-lactams in question were converted into their respective thiono equivalents **1b**−**5b**, by thionation reaction with Lawesson's reagent.[14a,28] It is well-known that in the thiocarbonyl compounds, in general, the UV and ECD bands are shifted appreciably to the red.[28b,29] The sign of the n → π^* band for amides and thioamides is the same providing that their chiral environment remains identical. The UV spectra of compounds **1b**−**5b** show a weak low-energy band around 330 nm corresponding to the n → π^* transition, the intense band at around 260 nm arising from the π → π^* excitation, and a moderately intense band at ca. 210 nm (Table 4).[4i] The polarization direction of this short-wavelength transition, most probably of an n_σ → π^* origin[28b,29] is nearly orthogonal to the polarization direction of the π → π^* band.

In variable low-temperature ECD spectra the intensity of the diagnostic band is greatly dependent on the temperature of the solution (Figure 7). In most cases, the 340 nm band, associated with n → π^* thioamide transition, shows increase in intensity with lowering temperature (Figure 7). This strongly indicates that most of the molecules are frozen in the preferred conformation. Much smaller temperature dependence is observed in the case of compound **4b**. The results, however, are in line with the calculations, because the population of the lowest energy conformer with computed CE in the corresponding spectral regions should increase with decreasing temperature.

Additional evidence comes from the X-ray diffraction results of compound **1b**, the only one forming suitable crystals for such

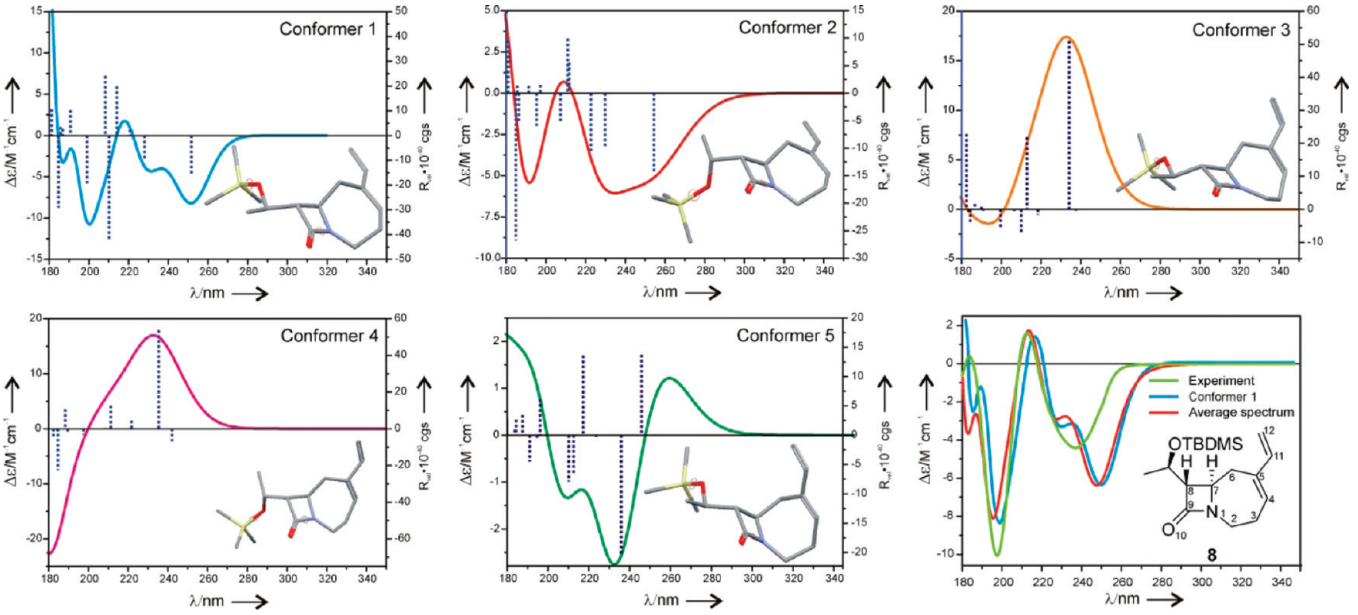

Figure 6. COSMO-BLYP-D/def-TZVP structures of conformers of β-lactam **8** and their computed ECD spectra at the TD-PBE0/def2-TZVPP level of theory, together with the Boltzmann-averaged spectrum compared to experiment. The symbol ε denotes the molar decadic absorption coefficient, and λ is the excitation wavelength.

Table 4. UV and ECD Data of β-Lactams 1b−5b Recorded in Acetonitrile at Room Temperature

compd	UV ε (λ_{max}); [$M^{-1}cm^{-1}$(nm)]			CD $\Delta\varepsilon$ (λ_{max}); [$M^{-1}cm^{-1}$(nm)]			
1b	5500 (212)	15000 (265)	60 (326)	−2.3 (208.0)[a]	+8.87 (265.0)	−1.1 (280.5)	−1.8 (328.0)
2b	7100 (210)	17900 (266)	90 (325)	+17.4 (210.0)		−1.1 (277.5)	−2.6 (330.5)
3b	6700 (206^{sh})	16100 (262)	70 (333)	+20.5 (200.5)		−4.6 (266.0)	−5.7 (335.0)
4b	6900 (207^{sh})	14000 (270)	75 (329)	+49.7 (198.0)[b]	−6.1 (252.0)	−9.2 (272.5)	−2.2 (336.0)
5b	7000 (211)	14100 (265)	70 (325)	−4.5 (193.5)[c]	+9.2 (201.5)	+6.8 (264.0)	−3.7 (331.0)

[a] An additional small positive ECD band is observed at around 220 nm. [b] An additional small negative ECD band is observed at around 220 nm. [c] An additional small positive ECD band is observed at around 212 nm.

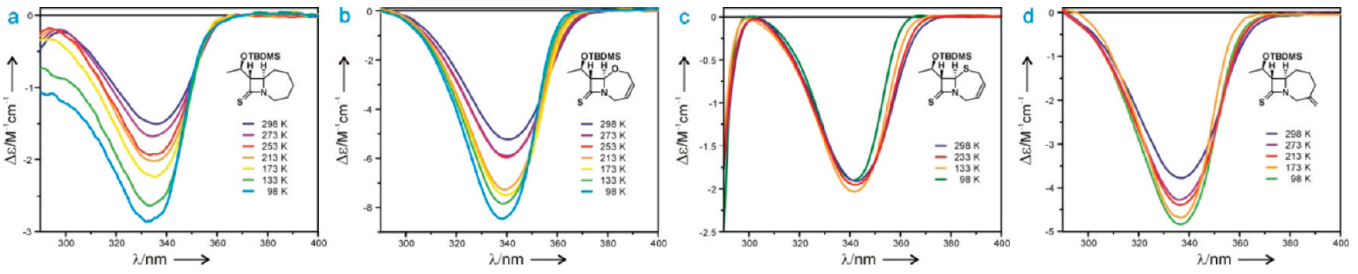

Figure 7. Variable low-temperature ECD spectra of β-lactams **1b** (a), **3b** (b), **4b** (c), and **5b** (d) recorded in EPA (ether/isopentane/ethanol, 5:5:2 by vol).

analysis (Figure 8). The structural data clearly demonstrate the planarity of the amide chromophore and the chair form of seven-membered ring. Additionally, the dihedral angle C9−C7−C2−N equals to −2.0°, which quantifies the sp^2 hybridization of the amide nitrogen atom.

The excellent agreement between the solid-state structure and the computed one (Table 5), as well as the close similarity of the ECD spectra of **1b** recorded in both solid-state and solution (Figure 8), indicates the presence of the same molecular species in both states. This means that the solute−solvent interactions, which may considerably affect the CD spectra owing to both conformational and vicinal effects, are negligible in these cases and indicate that the observed ECD is largely a molecular property. Therefore, the analysis of the ECD data can be performed on the basis of chiroptical data obtained for solutions.

In addition, the literature data for tricyclic β-lactam analogues, structurally very similar to our model compound **5a,** confirm the planarity of amide chromophore in such cyclic systems.[30] Torsion angles S10−C9−N−C2 and S10−C9−N−C7, taken from ref 31, equal to 4.3° and 176.4°, respectively, demonstrate the

dx.doi.org/10.1021/jo200171w |J. Org. Chem. 2011, 76, 3306–3319

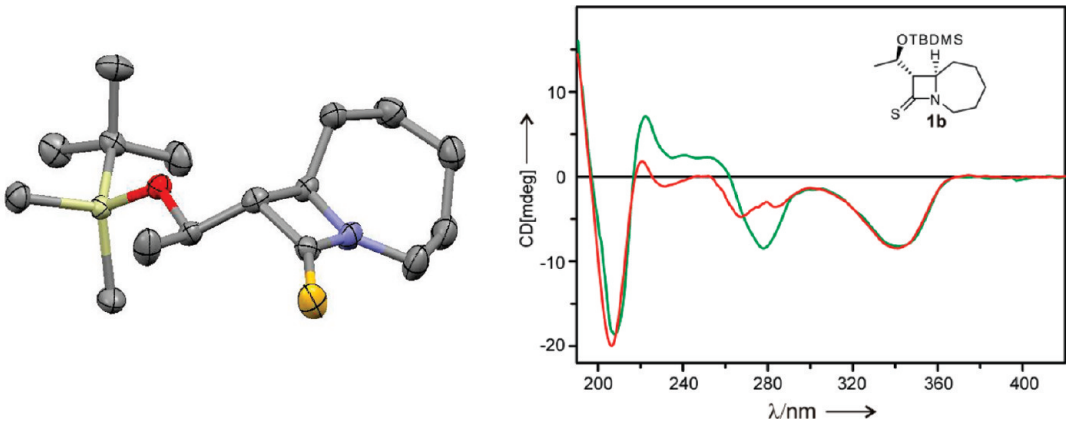

Figure 8. (Left) ORTEP diagram of compound **1b**. Thermal ellipsoids are shown at 50% probability level. Hydrogen atoms are omitted for clarity. (Right) ECD spectra of β-lactam **1b** recorded in MI13 (methylcyclohexane/isopentane, 1:3, by vol) (green line) and nujol mull (red line) given in μdeg.

Table 5. Torsion Angles in Degrees and Pyramidal Height in pm of Compound 1b in Comparison with the Lowest Energy COSMO-BLYP-D/def2-TZVP Conformer Structure

	torsion angle[a]										
	1	2	3	4	5	6	7	8	9	10	pyramidal height
X-ray	−0.7	+176.4	+178.8	+61.1	−84.8	+67.8	−62.9	+72.1	−61.8	+2.6	−2.1
BLYP-D	−1.9	+179.9	−179.1	+62.9	−85.3	68.2	−64.5	+73.0	−59.3	−1.5	+0.01

[a] Torsion angles: 1 = S10−C9−N−C2; 2 = S10−C9−N−C7; 3 = C9−N−C2−C3; 4 = N−C2−C3−C4; 5 = C2−C3−C4−C5; 6 = C3−C4−C5−C6; 7 = C4−C5−C6−C7; 8 = C5−C6−C7−N; 9 = C6−C7−N−C2; 10 = C7−N−C2−C3.

planarity of the chromophoric system in these tricyclic β-lactams and are in full agreement with our results for **1b**. Thus, we can conclude that the nonclassical β-lactams with a seven-membered ring fused together with an azetidinone ring do not obey the helicity rule.

3. CONCLUSIONS

The relationship between the molecular structure and the chiroptical properties of nonclassical β-lactams **1**−**10** was investigated by electronic circular dichroism spectroscopy, variable low-temperature CD measurements, time-dependent density functional theory, and X-ray diffraction analysis. The computed O10−C9−N1−C2 and O10−C9−N1−C7 torsion angles provide corroborating evidence for the planarity of amide chromophore. Thus, the β-lactam analogues examined in this work do not conform to the previously established helicity rule. However, this fact does not constitute an exception to the rule because this rule was formulated strictly for β-lactam analogues with a nonplanar amide chromophore only, whereas in the studied systems the chromophore is planar.

TD-PBE0 calculations of ECD spectra are in good agreement with the corresponding experimental data and allow an assignment of the absolute configuration at the ring junction in β-lactams **1**−**10**. In calculations it was necessary to consider five to seven conformers of each compound. The obtained results have shown that the sign of ECD band at 220 nm, characteristic for β-lactams, is closely related to the stereostructure of the chromophoric system. This band has mainly the character of an amide n(O) $\rightarrow \pi^*$ transition.

The study demonstrated a high sensitivity of the ECD spectra for even the smallest conformational differences caused by the substitution of the seven-membered ring and the side-chain flexibility. The presence of an additional, interfering chromophore in the molecule complicates interpretation of results. Nevertheless, it is demonstrated that even in such cases the experimental ECD spectroscopy supported by computational results can be successfully utilized in context of the configurational and conformational analysis of two- and multifunctional bi- and polycyclic β-lactams with one or more stereogenic centers. We strongly recommend such a combined analysis of chiroptical properties because it can provide detailed insight in the three-dimensional structure and conformational dynamics of chiral molecules.

4. EXPERIMENTAL SECTION

4.1. General Information. ^{1}H and ^{13}C NMR spectra were recorded on 200 or 500 MHz spectrometers in $CDCl_3$ at ambient temperatures. Chemical shifts (δ) are reported in parts per million, using residual solvents as internal standard. Optical rotations were measured in CH_2Cl_2 solutions at ambient temperature and are quoted in units of 10^{-1} deg cm^2 g^{-1}. Infrared spectra were obtained using neat samples on FTIR (ATR) spectrometer. Electrospray ionization (ESI) mass spectrometry (MS) experiments were performed on a spectrometer under normal conditions. PFK solution was used as calibrant for HRMS measurements. UV spectra were measured using acetonitrile as a solvent. CD spectra were recorded between 180 and 400 nm at room temperature using acetonitrile solutions. Solutions with concentrations in the range 0.8×10^{-4} to 1.2×10^{-3} mol dm^{-3} were examined in cells with path length 0.1 or 1 cm. Low-temperature ECD measurements were recorded with a spectropolarimeter equipped with a cryostat using MI-13 (methylcyclopentane/'isooctane 1:3 by vol) or EPA (ether/isopentane/ethanol 5:5:2 by vol) as solvents.

dx.doi.org/10.1021/jo200171w |J. Org. Chem. 2011, 76, 3306–3319

HPLC separation of mixture of lactams **6** and **7** was performed on Kromasil 100 Si (5 μ) column, with hexane/isopropanol (9:1) as a mobile phase.

All reactions were monitored by thin-layer chromatography using gel plates 60 F254; visualization was accomplished with UV light and/or staining with appropriate stains ($KMnO_4$, anisaldehyde, vaniline, ninhydrin, or phosphomolybdic acid). Standard flash chromatography procedures were followed (particle size 40−63 μm).

4.2. Materials. Commercially available starting materials were used without further purification. Solvents were purified according to the literature methods before use.[31] All of the spectral data for known compounds either match those reported or by comparison to the literature report.

4.3. Synthesis of Investigated Compounds.

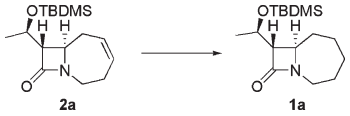

*(7R,8S)-8-[(1R)-(tert-Butyl-dimethyl-silanyloxy)-ethyl]-1-aza-bicyclo-[5.2.0]nonan-9-one (**1a**).* A mixture of **2a** (50 mg, 0.17 mmol), 10% Pd on charcoal (5 mg), and ethanol (10 mL) was placed in a 50 mL round-bottom flask equipped with a magnetic stirring bar, and the flask was attached to an atmospheric pressure hydrogenation apparatus. Then the flask was filled with hydrogen, and the components were vigorously stirred until uptake of hydrogen had been ceased (ca. 2.1 mL). Then the mixture was filtered through Celite, and the solvent was evaporated to yield analytically pure **1a** (47 mg, 95%) as a colorless oil. $[\alpha]_D$ −11.2 (*c* 0.54, CH_2Cl_2). IR (film) ν/cm^{-1}: 1750, 1472, 1398, 1256. ^{1}H NMR (500 MHz, $CDCl_3$) δ/ppm: 0.058 (s, 3H), 0.061 (s, 3H), 0.86 (s, 9H), 1.20 (d, *J* = 6.3 Hz, 3H), 1.29−1.39 (m, 2H), 1.40−1.55 (m, 2H), 1.82−1.92 (m, 3H), 2.60 (d, *J* = 5.1 Hz, 1H), 3.25 (dt, *J* = 13.0, 4.3 Hz, 1H), 3.33 (tdd, *J* = 13.0, 3.5, 1.2 Hz, 1H), 3.66 (dt, *J* = 9.9, 2.2 Hz, 1H), 4.14 (dq, *J* = 6.3, 5.2 Hz, 1H). ^{13}C NMR (125 MHz, $CDCl_3$) δ/ppm: −5.0, −4.2, 17.9, 22.6, 25.7 (3C), 26.7, 28.7, 29.4, 35.3, 42.6, 55.65, 62.2, 65.7, 167.4. HR MS (ESI) calcd for $[M + Na]^+$ $C_{16}H_{31}NO_2NaSi$ 320.2016, found 320.2023.

General Procedure for Thionation of β-Lactams with Lawesson's Reagent. A solution of β-lactam (**1a**, **2a**, **3a**, **4a**, or **5a**) (0.1 mmol) and Lawesson's reagent (0.05 mmol) in benzene (10 mL) was refluxed for 2 h. Then the solvent was removed and the crude product was purified by chromatography on silica gel to produce thionation product (**1b**, **2b**, **3b**, **4b**, or **5b**).

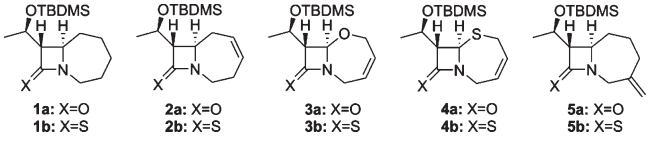

*(7R,8S)-8-[(1R)-(tert-Butyl-dimethyl-silanyloxy)-ethyl]-1-aza-bicyclo-[5.2.0]nonane-9-thione (**1b**).* Chromatographed using 5% AcOEt in hexane, colorless crystals, mp 29−32 °C, yield 80%. $[\alpha]_D$ −10.3 (*c* 0.51, CH_2Cl_2). IR (film) ν/cm^{-1}: 1492, 1461, 1449, 1373, 1291. ^{1}H NMR (500 MHz, $CDCl_3$) δ/ppm: 0.081 (s, 3H), 0.084 (s, 3H), 0.86 (s, 9H), 1.26 (d, *J* = 6.3 Hz, 3H), 1.30−1.39 (m, 2H), 1.52−1.62 (m, 2H), 1.88−1.94 (m, 3H), 1.96−2.05 (m, 3H), 2.56−2.59 (m, 1H), 3.45−3.57 (m, 2H), 4.15−4.22 (m, 2H). ^{13}C NMR (125 MHz, $CDCl_3$) δ/ppm: −4.7, −3.9, 17.9, 22.3, 25.8(3C), 25.9, 29.0, 29.4, 34.4, 46.5, 63.1, 64.6, 66.3, 199.83 HR MS (ESI) calcd for $[M + Na]^+$ $C_{16}H_{31}NO$-NaSiS 336.1788, found 336.1783.

*(7R,8S)-8-[(1R)-(tert-Butyl-dimethyl-silanyloxy)-ethyl]-1-aza-bicyclo-[5.2.0]non-4-en-9-thione (**2b**).* Chromatographed using 5% AcOEt in hexane, colorless oil, yield 79%. $[\alpha]_D$ 29.3 (*c* 0.35, CH_2Cl_2). IR (film) ν/cm^{-1}: 1495, 1442, 1271, 1257, 1139, 836, 777. ^{1}H NMR (500 MHz, $CDCl_3$) δ/ppm: 0.08 (s, 3H), 0.09 (s, 3H), 0.86 (s, 9H), 1.29 (d, *J* = 6.4 Hz, 3H), 2.29−2.47 (m, 2H), 2.71 (d, *J* = 4.6 Hz, 1H), 3.67 (bd, *J* = 18.9 Hz, 1H), 3.99 (dd, *J* = 9.6, 5.7 Hz, 1H), 4.23 (qd, *J* = 6.2, 4.9 Hz, 1H), 4.32−4.41 (m, 1H), 5.74−5.80 (m, 1H), 5.83−5.90 (m, 1H). ^{13}C NMR (125 MHz, $CDCl_3$) δ/ppm: −4.7, −4.0, 17.9, 22.4, 25.8(3C), 28.0, 41.0, 54.4, 66.1, 67.8, 122.0, 123.8, 200.7. HR MS (ESI) calcd for $[M + Na]^+$ $C_{16}H_{29}NONaSiS$ 334.16314, found 334.16349.

*(7R,8R)-8-[(1R)-(tert-Butyl-dimethyl-silanyloxy)-ethyl]-6-oxa-1-aza-bicyclo[5.2.0]non-3-en-9-thione (**3b**).* Chromatographed using 5% AcOEt in hexane, colorless oil, yield 87%. $[\alpha]_D$ −92.24 (*c* 0.56, CH_2Cl_2). IR (film) ν/cm^{-1}: 1490. ^{1}H NMR (500 MHz, $CDCl_3$) δ/ppm: 0.10 (s, 3H), 0.11 (s, 3H), 0.88 (s, 9H), 1.31 (d, *J* = 6.4 Hz, 3H), 3.02 (bs, 1H), 3.84−3.91 (m, 1H), 4.25−4.33 (m, 2H), 4.43−4.50 (m, 1H), 4.71−4.79 (m, 1H), 5.60 (s, 1H), 5.63−5.73 (m, 2H). ^{13}C NMR (125 MHz, $CDCl_3$) δ/ppm: −4.7, −4.0, 17.9, 22.2, 25.8(3C), 44.8, 64.8, 65.4, 66.6, 90.4, 124.2, 128.6, 200.5. HR MS (LSI) calcd for $[M + Na]^+$ $C_{15}H_{27}NO_2NaSiS$: 336.1424, found 336.1410. Elemental Analysis calcd for $C_{15}H_{27}NO_2SiS$: C, 57.46; H, 8.68; N, 4.47. Found: C, 57.60; H, 8.89; N, 4.27.

*(7R,8S)-8-[(1R)-(tert-Butyl-dimethyl-silanyloxy)-ethyl]-6-thia-1-aza-bicyclo[5.2.0]non-3-en-9-thione (**4b**).* Chromatographed using 5% AcOEt in hexane, colorless oil, yield 90%. $[\alpha]_D$ −20.6 (*c* 0.50, $CDCl_3$). IR (film) ν/cm^{-1}: 1481. ^{1}H NMR (500 MHz, $CDCl_3$) δ/ppm: 0.08 (s, 3H), 0.09 (s, 3H), 0.85 (s, 9H), 1.27 (d, *J* = 6.3 Hz, 3H), 2.99 (dd, *J* = 16.7, 8.3 Hz, 1H), 3.07 (dd, *J* = 3.1, 1.4 Hz, 1H), 3.39−3.45 (m, 1H), 3.85 (dq, *J* = 17.8, 2.7 Hz, 1H), 4.32 (qd, *J* = 6.3, 3.1 Hz, 1H), 4.80 (ddt, *J* = 17.8, 5.1, 1.6 Hz, 1H), 5.38 (s, 1H), 5.56 (ddt, *J* = 11.1, 5.1, 2.3 Hz, 1H), 5.90−5.96 (m, 1H). ^{13}C NMR (125 MHz, $CDCl_3$) δ/ppm: 17.9, 22.0, 24.3, 25.8(3C), 44.1, 64.9, 65.3, 67.3, 126.2, 129.7, 200.8. HR MS (ESI) calcd for $[M + Na]^+$ $C_{15}H_{27}NONaSiS_2$ 352.11956, found 352.12118.

*(7R,8S)-8-[(1R)-(tert-Butyl-dimethyl-silanyloxy)-ethyl]-3-methylene-1-aza-bicyclo[5.2.0]nonan-9-thione (**5b**).* Chromatographed using 5% AcOEt in hexane, colorless oil, yield 80%. $[\alpha]_D$ 25.4 (*c* 0.50, CH_2Cl_2). IR (film) ν/cm^{-1}: 1485, 1442, 1258, 1248, 1140, 1093, 836, 776.^{1}H NMR (500 MHz, $CDCl_3$) δ/ppm: 0.07 (s, 3H), 0.08 (s, 3H), 0.85 (s, 9H), 1.25 (d, *J* = 6.3 Hz, 3H), 1.33−1.44 (m, 1H), 1.49−1.61 (m, 2H), 1.90 (td, *J* = 12.9, 2.7 Hz, 1H), 1.99−2.07 (m, 2H), 2.59−2.66 (m, 2H), 3.86 (d, *J* = 15.1 Hz, 1H), 4.11 (bd, *J* = 11.6 Hz, 1H), 4.18 (qd, *J* = 6.3, 4.3 Hz, 1H), 4.29 (bd, *J* = 15.1 Hz, 1H), 5.02 (t, *J* = 1.6 Hz, 1H), 5.05 (bs, 1H). ^{13}C NMR (125 MHz, $CDCl_3$) δ/ppm: 17.8, 22.3, 25.8(3C), 29.9, 34.6, 36.7, 52.8, 63.9, 64.3, 66.2, 118.0, 143.1, 200.2. HR MS (ESI) calcd for $[M + Na]^+$ $C_{17}H_{31}NONaSiS$ 348.17879, found 348.1803.

General Procedure for Metathesis Reaction. A mixture of lactam (**13a**, **13b**, **13c**, **19**, **21**, or **23**) (0.62 mmol), anhydrous dichloromethane (25 mL), and Grubbs' first or second ruthenium catalyst (0.03 mmol) was refluxed under an argon atmosphere until the substrate had disappeared (according to TLC). Then the solvent was removed, and the residue was purified by chromatography on silica gel to produce cyclic product (**2a**, **3a**, **4a**, **8**, **9**, or **10**).

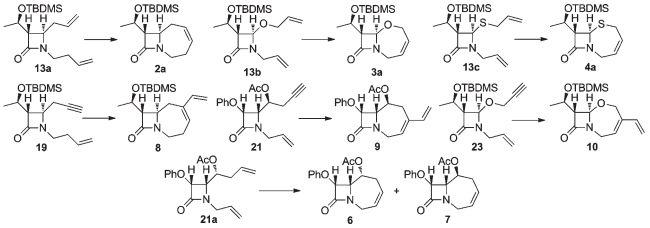

*(7R,8S)-8-[(1R)-(tert-Butyl-dimethyl-silanyloxy)-ethyl]-1-aza-bicyclo-[5.2.0]non-4-en-9-one (**2a**).* Catalyst - Grubbs' first, reaction time 1 h,

chromatographed using 10% AcOEt in hexane, colorless oil, yield 70%. $[\alpha]_D$ −12.2 (*c* 0.62, CH_2Cl_2). IR (film) ν/cm^{-1}: 1753, 142, 835, 777. ^1H NMR (500 MHz, $CDCl_3$) δ/ppm: 0.05 (s, 3H), 0.06 (s, 3H), 0.86 (s, 9H), 1.21 (d, *J* = 6.2 Hz, 3H), 2.15−2.21 (m, 1H), 2.33−2.42 (m, 3H), 2.74−2.81 (m, 2H), 3.55−3.58 (m, 1H), 3.76 (ddd, *J* = 13.3, 5.3, 3.5 Hz, 1H), 4.14 (dq, *J* = 6.2, 5.3 Hz, 1H), 5.85−5.95 (m, 2H). ^{13}C NMR (125 MHz, $CDCl_3$) δ/ppm: −5.0, −4.2, 17.9, 22.6, 25.7(3C), 27.7, 33.8, 39.2, 52.9, 63.9, 65.6, 129.8, 131.5, 166.3. HR MS (ESI) calcd for $[M + Na]^+$ $C_{16}H_{29}NO_2NaSi$ 318.1860, found 318.1875.

*(7R,8R)-8-[(1R)-(tert-Butyl-dimethyl-silanyloxy)-ethyl]-6-oxa-1-aza-bicyclo[5.2.0]non-3-en-9-one (**3a**).* Catalyst - Grubbs' first, reaction time 2 h, chromatographed using 10% AcOEt in hexane, colorless oil, yield 81%. $[\alpha]_D$ 62.4 (*c* 0.50, $CHCl_3$). IR (film) ν/cm^{-1}: 1768. ^1H NMR (500 MHz, $CDCl_3$) δ/ppm: 0.06 (s, 3H), 0.08 (s, 3H), 0.87 (s, 9H), 1.26 (d, *J* = 6.3 Hz, 3H), 3.05 (bd, *J* = 3.4 Hz, 1H), 3.66−3.73 (m, 1H), 4.18−4.24 (m, 2H), 4.36−4.46 (m, 2H), 5.23 (s, 1H), 5.56−5.61 (m, 1H), 5.63−5.68 (m, 1H). ^{13}C NMR (125 MHz, $CDCl_3$) δ/ppm: −5.2, −4.2, 17.9, 22.4, 24.3, 25.7(3C), 41.1, 57.9, 64.6, 66.7, 127.5, 133.2, 166.3. Elemental Analysis calcd for $C_{15}H_{27}NO_3Si$: C, 57.46; H, 8.68; N, 4.47. Found: C, 57.60; H, 8.89; N, 4.27.

*(7R,8S)-8-[(1R)-(tert-Butyl-dimethyl-silanyloxy)-ethyl]-6-thia-1-aza-bicyclo[5.2.0]non-3-en-9-one (**4a**).* Catalyst - Grubbs' first, reaction time 5 h, chromatographed using 10% AcOEt in hexane, colorless oil, yield 81%. $[\alpha]_D$ 31.2 (*c* 0.51, CH_2Cl_2). IR (film) ν/cm^{-1}: 1762, 836, 778. ^1H NMR (500 MHz, $CDCl_3$) δ/ppm: 0.05 (s, 3H), 0.08 (s, 3H), 0.87 (s, 9H), 1.22 (d, *J* = 6.30 Hz, 3H), 2.99 (dd, *J* = 16.39, 8.04 Hz, 1H), 3.15 (dd, *J* = 3.80, 1.74 Hz, 1H), 3.45−3.50 (m, 1H), 3.63−3.68 (m, 1H), 4.20−4.25 (m, 1H), 4.33 (dd, *J* = 18.1, 5.29 Hz, 1H), 4.90 (s, 1H), 5.50−5.56 (m, 1H), 5.93−5.96 (m, 1H). ^{13}C NMR (125 MHz, $CDCl_3$) δ/ppm: −5.0, −4.2, 18.2, 22.5, 24.7, 25.8(3C), 41.3, 58.4, 65.2, 67.1, 128.0, 130.6, 166.3. HR MS (ESI) calcd for $[M + Na]^+$ $C_{15}H_{27}NO_2NaSiS$ 336.1424, found 336.14233.

*Acetic Acid (6R,7S,8R)-9-Oxo-8-phenoxy-1-aza-bicyclo[5.2.0]non-3-en-6-yl Ester (**6**) and Acetic Acid (6S,7S,8R)- 9-Oxo-8-phenoxy-1-aza-bicyclo[5.2.0]non-3-en-6-yl ester (**7**).* Catalyst - Grubb's first, reaction time 2.5 h, chromatographed using 10% acetone in hexane, colorless oil, yield 86%. Sample of the mixture (5 mg) was separated using HPLC (detection at 202 nm, column Kromasil 100 Si (5 μ) 25 × 0.4 cm, 10% iPrOH in hexane, flow 1 mL/min) yielding compound **6** (t_R = 13.1 min, 2.94 mg) and 7 (t_R = 11.1 min, 0.98 mg). **Data for 6**: $[\alpha]_D$ 63.9 (*c* 0.64, CH_2Cl_2). IR (film) ν/cm^{-1}: 1764, 1737, 1597, 1489, 1241. ^1H NMR (500 MHz, $CDCl_3$) δ/ppm: 1.80 (s, 3H), 2.49−2.51 (m, 1H), 2.71−2.81 (m, 1H), 3.63 (d, *J* = 17.5 Hz, 1H), 4.12 (dd, *J* = 5.9, 4.2 Hz, 1H), 4.46 (dd, *J* = 17.5, 4.2 Hz, 1H), 5.19 (ddd, *J* = 8.3, 5.9, 2.4 Hz, 1H), 5.39 (d, *J* = 4.2 Hz, 1H), 5.62−5.70 (m, 2H), 6.98−7.05 (m, 3H), 7.24−7.32 (m, 2H). ^{13}C NMR (125 MHz, $CDCl_3$) δ/ppm: 20.9, 32.5, 41.6, 60.1, 68.5, 80.3, 115.2(2C), 122.2, 124.7, 125.2, 129.6(2C), 157.6, 165.8, 170.2. HR MS (ESI) calcd for $[M + Na]^+$ $C_{16}H_{17}NO_4Na$ 310.1049, found 310.1037. **Data for 7**: $[\alpha]_D$ 60.5 (*c* 0.45, CH_2Cl_2). IR (film) ν/cm^{-1}: 1764, 1737, 1597, 1489, 1241. ^1H NMR (500 MHz, $CDCl_3$) δ/ppm: 1.89 (s, 3H), 2.43 (d, *J* = 17.7 Hz, 1H), 2.88−2.94 (m, 1H), 3.73 (d, *J* = 19.1 Hz, 1H), 4.22 (dd, *J* = 4.2, 2.5 Hz, 1H), 4.53 (dd, *J* = 19.1, 2.4 Hz, 1H), 5.33 (d, *J* = 4.2 Hz, 1H), 5.41 (ddd, *J* = 6.6, 2.5, 2.4 Hz, 1H), 5.56−5.59 (m, 2H), 6.97−7.03 (m, 3H), 7.25−7.33 (m, 2H). ^{13}C NMR (125 MHz, $CDCl_3$) δ/ppm: 20.6, 31.1, 40.6, 62.2, 70.7, 81.1, 115.4(2C), 122.3, 125.3, 127.1, 129.5(2C), 157.4, 164.5, 169.7. HR MS (ESI) calcd for $[M + Na]^+$ $C_{16}H_{17}NO_4Na$ 310.1049, found 310.1037.

*(7R,8S)-8-[(1R)-(tert-Butyl-dimethyl-silanyloxy)-ethyl]-5-vinyl-1-aza-bicyclo[5.2.0]non-4-en-9-one (**8**).* Catalyst - Grubbs' first, reaction time 9 h, chromatographed using 10% AcOEt in hexane, colorless oil, yield 60%. IR (film) ν/cm^{-1}: 1751, 1410, 1256, 1143, 835. ^1H NMR (500 MHz, $CDCl_3$) δ/ppm: 0.05 (s, 3H), 0.07 (s, 3H), 0.91 (s, 9H), 1.25 (d, *J* = 6.2 Hz, 3H), 2.22−2.29 (m, 1H), 2.40−2.47 (m, 2H), 2.72−2.82 (m, 2H), 2.83 (dd, *J* = 6.2 Hz, 1.8, 1H), 3.45 (dt, *J* = 10.9, 2.1 Hz, 1H), 3.80 (ddd, *J* = 13.3, 5.1, 3.6 Hz, 1H), 4.11 (qui, *J* = 6.2 Hz, 1H), 5.05 (d, *J* = 10.8 Hz, 1H), 5.15 (d, *J* = 17.4 Hz, 1H), 5.96 (t, *J* = 7.2 Hz, 1H), 6.35 (dd, *J* = 17.4, 10.8 Hz, 1H). ^{13}C NMR (125 MHz, $CDCl_3$, δ/ppm) −5.0, −4.2, 17.9, 22.7, 25.7(3C), 27.6, 31.5, 38.7, 52.9, 64.1, 66.1, 111.8, 131.7, 139.4, 140.5, 166.4. HR MS (ESI) calcd for $[M + Na]^+$ $C_{18}H_{31}NO_2NaSi$ 344.2009, found 344.2031.

*Acetic Acid (6S,7S,8R)-9-oxo-8-phenoxy-4-vinyl-1-aza-bicyclo[5.2.0]non-3-en-6-yl Ester (**9**).* Catalyst - Grubbs' second, reaction time 1.5 h, chromatographed using 15−20% AcOEt in hexane, colorless oil, yield 92%. $[\alpha]_D$ 74.1 (*c* 0.84, CH_2Cl_2). IR (film) ν/cm^{-1}: 1764, 1743, 1599, 1495, 1244. ^1H NMR (500 MHz, $CDCl_3$) δ/ppm: 1.84 (s, 3H), 2.54 (dd, *J* = 16.8, 1.7 Hz, 1H), 3.15 (ddt, *J* = 16.8, 7.9, 1.5 Hz, 1H), 3.77−3.83 (m, 1H), 4.23 (dd, *J* = 4.4, 2.8 Hz, 1H), 4.52−4.58 (m, 1H), 5.01 (d, *J* = 10.9 Hz, 1H), 5.15 (d, *J* = 17.3 Hz, 1H), 5.35 (dd, *J* = 4.4, 1.1 Hz, 1H), 5.68−5.71 (m, 1H), 6.32 (dd, *J* = 17.3, 10.9 Hz, 1H), 6.97−7.03 (m, 3H), 7.27−7.31 (m, 2H). ^{13}C NMR (125 MHz, $CDCl_3$) δ/ppm: 20.8, 30.2, 40.4, 59.9, 67.4, 80.8, 112.5, 115.2(2C), 122.2, 126.4, 129.6(2C), 135.4, 140.9, 157.6, 165.6, 170.2. HR MS (ESI) calcd for $[M + Na]^+$ $C_{18}H_{19}NO_4Na$ 336.1206, found 336.1198.

*(3R,4R)-8-[(1R)-(tert-Butyl-dimethyl-silanyloxy)-ethyl]-4-vinyl-6-oxa-1-aza-bicyclo[5.2.0]non-3-en-9-one (**10**).* Catalyst - Grubbs' first, reaction time 1.5 h, chromatographed using 15% AcOEt in hexane, colorless oil, yield 80%. IR (film) ν/cm^{-1}: 1767, 1737, 1645, 1472, 1252. ^1H NMR (500 MHz, $CDCl_3$) δ/ppm: 0.06 (s, 3H), 0.08 (s, 3H), 0.86 (s, 9H), 1.27 (d, *J* = 6.3 Hz, 3H), 3.07 (d, *J* = 3.5 Hz, 1H), 3.77 (d, *J* = 1958 Hz, 1H), 4.22 (dq, *J* = 6.3, 3.5 Hz, 1H), 4.37 (dd, *J* = 15.6, 1.2 Hz, 1H), 4.46 (dd, *J* = 19.5, 4.8 Hz, 1H), 4.62 (d, *J* = 15.6 Hz, 1H), 5.03 (dd, *J* = 11.2, 0.6 Hz, 1H), 5.10 (d, *J* = 17.7 Hz, 1H), 5.27 (s, 1H), 5.63 (dd, *J* = 4.0, 3.3 Hz, 1H), 6.25 (dd, *J* = 17.7, 11.2 Hz). ^{13}C NMR (125 MHz, $CDCl_3$) δ/ppm: −5.2, −4.3, 17.9, 22.5, 25.6(3C), 40.9, 63.6, 64.0, 64.3, 84.5, 112.3, 127.4, 138.3, 138.4, 165.9. HR MS (ESI) calcd for $[M + Na]^+$ $C_{17}H_{29}NO_3NaSi$ 346.1809, found 346.1822.

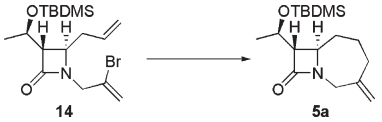

*(7R,8S)-8-[(1R)-(tert-Butyl-dimethyl-silanyloxy)-ethyl]-3-methylene-1-aza-bicyclo[5.2.0]nonan-9-one (**5a**).* A solution of tributyltinhydride (107 mg, 0.37 mmol) in benzene (1 mL) was added within 1 h to boiling solution of β-lactam **14** (80 mg, 0.21 mmol) and AIBN (23 mg, 0.14 mmol) in benzene (9 mL). Then the benzene was evaporated, and the residue was chromatographed on silica gel (gradient 5−15% AcOEt in hexane) to produce cyclic product as colorless oil (51 mg, 80%). $[\alpha]_D$ 31.3 (*c* 0.57, CH_2Cl_2). IR (film) ν/cm^{-1}: 1754. ^1H NMR (500 MHz, $CDCl_3$) δ/ppm: 0.05 (s, 6H), 0.85 (s, 9H), 1.18 (d, *J* = 6.3 Hz, 3H), 1.31−1.45 (m, 2H), 1.87−1.94 (m, 1H), 1.94−2.04 (m, 2H), 3.55 (dt, *J* = 10.6, 2.1 Hz, 1H), 3.69 (d, *J* = 13.9 Hz, 1H), 4.09 (bd, *J* = 13.9 Hz, 1H), 4.15 (qd, *J* = 6.2, 4.7 Hz, 1H), 4.91 (bs, 1H), 4.94 (bs, 1H). ^{13}C NMR (125 MHz, $CDCl_3$) δ/ppm: −5.0, −4.2, 17.84, 22.6, 25.7(3C), 29.9, 35.7, 36.5, 49.2, 55.3, 63.2, 65.5, 116.2, 144.6, 167.5. HR MS (LSI) calcd for $[M + Na]^+$ $C_{17}H_{31}NO_2NaSi$ 332.2016, found 332. 2023.

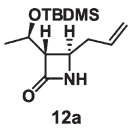

*(3S,4R)-4-Allyl-3-[(1R)-(tert-butyl-dimethyl-silanyloxy)-ethyl]-azetidin-2-one (**12a**)*[13]. A mixture of potassium iodide (1.74 g, 10.5 mmol),

allyl bromide (0.88 mL, 10.5 mmol) and powdered indium (0.79 g, 6.94 mmol) in DMF (40 mL) was stirred for 1 h. Then the solution of compound **11** (1 g, 3.46 mmol) in DMF (10 mL) was added and the stirring was continued at room temperature for 24 h. Then the insoluble material was filtered off and washed with diethyl ether. The filtrate was poured into ammonium chloride and extracted with diethyl ether. The organic layer was washed with brine and dried over $MgSO_4$. Then the solvent was evaporated, and the residue was purified by chromatography on silica gel (10−20% AcOEt in hexane) to produce **12a** (807 mg, 86%). $[\alpha]_D$ +8.67 (*c* 0.67, CH_2Cl_2). IR (film) ν/cm^{-1}: 1760. Elemental Analysis calcd for $C_{14}H_{27}NO_2SiS$: C, 62.40; H, 10.10; N, 5.20, Found: C, 62.60; H, 10.22; N, 5.32. HR MS (LSI) calcd for $[M + Na]^+$ $C_{14}H_{27}NO_2NaSi$ 292.17037, found 292.17026.

General Procedure for N-Alkylation of *β*-Lactams with 4-Bromo-1-butene. A mixture of compound **12a** or **18** (1.56 mmol), potassium iodide (0.13 mmol), Bu_4NHSO_4 (0.58 mmol), THF (15 mL), powdered potassium hydroxide (3.6 mmol), and 4-bromo-1-butene (3.6 mmol) was stirred at room temperature in the argon atmosphere for 24 h. Then the insoluble material was filtered off and washed with THF. The filtrate was washed with ammonium chloride, brine and dried over $MgSO_4$. Then the solvent was evaporated, and the residue was purified by chromatography on silica gel (5% acetone in hexane) to produce **13a** or **19**.

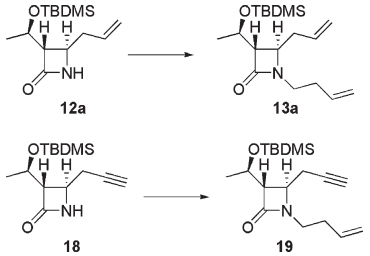

*(3S,4R)-4-Allyl-1-but-3-enyl-3-[(1R)-(tert-butyl-dimethyl-silanyloxy)-ethyl]-azetidin-2-one (**13a**).* Colorless oil, yield 60%. $[\alpha]_D$ −27.39 (*c* 0.81, CH_2Cl_2). IR (film) ν/cm^{-1}: 1754, 1642, 1472, 1405, 1256. ^1H NMR (500 MHz, $CDCl_3$) δ/ppm: 0.06 (s, 3H), 0.07 (s, 3H), 0.88 (s, 9H), 1.19 (d, *J* = 6.2 Hz, 3H), 2.25−2.36 (m, 3H), 2.46−2.52 (m, 1H), 2.74 (dd, *J* = 5.2, 1.9 Hz, 1H), 3.03−3.09 (m, 1H), 3.41 (ddd, *J* = 14.4, 8.0, 6.9 Hz, 1H), 3.66 (ddd, *J* = 7.2, 5.3, 2.0 Hz, 1H), 4.12 (quintet, *J* = 6.2 Hz, 1H), 5.04−5.19 (m, 4H), 5.73−5.84 (m, 2H). ^{13}C NMR (125 MHz, $CDCl_3$) δ/ppm: −4.8, −4.4, 17.9, 22.5, 25.8(3C), 32.7, 37.32, 4.8, 54,0, 62.4, 65.9, 116.9, 118.2, 133.5, 135.2, 167.7. HR MS (LSI) calcd for $[M + Na]^+$ $C_{18}H_{33}NO_2NaSi$ 346.21728, found 346. 21567.

*(3S,4R)-1-But-3-enyl-3-[(1R)-(tert-butyl-dimethyl-silanyloxy)-ethyl]-4-prop-2-ynyl-azetidin-2-one (**19**).* Colorless oil, yield 58%. IR (film) ν/cm^{-1}: 1755, 1642, 1472, 1257, 1142. ^1H NMR (500 MHz, $CDCl_3$) δ/ppm: 0.07 (s, 3H), 0.08 (s, 3H), 0.88 (s, 9H), 1.23 (d, *J* = 6.3 Hz, 3H), 2.05 (t, *J* = 2.6 Hz, 1H), 2.29−2.39 (m, 2H), 2.53−2.56 (m, 2H), 2.88 (dd, *J* = 4.8, 1.9 Hz, 1H), 3.12−3.18 (m, 1H), 3.42 (ddd, *J* = 14.5, 7.9, 6.9 Hz, 1H), 3.78 (dt, *J* = 5.4, 1.9 Hz, 1H), 4.16 (dq, *J* = 6.2, 6.1 Hz, 1H), 5.06 (dd, *J* = 10.2, 1.3 Hz, 1H), 5.11 (dd, *J* = 17.1, 1.6 Hz, 1H), 5.78 (ddt, *J* = 17.1, 10.2, 6.9 Hz, 1H). ^{13}C NMR (125 MHz, $CDCl_3$) δ/ppm: −4.8, −4.4, 17.9, 22.5, 22.8, 25.8(3C), 32.7, 40.0, 52.4, 62.6, 65.4, 71.2, 79.5, 116.9, 135.1, 167.4. HR MS (TOF FD+) calcd for $[M]^+$ $C_{18}H_{31}NO_2Si$ 321.2124, found 321.2114.

General Procedure for N-Alkylation of *β*-Lactams with Allyl Bromide. A mixture of lactam (**12b**, **12c**, **12a**, or **22**) (0.70 mmol), anhydrous DMF (12 mL) and sodium hydride (1.3 mmol) was stirred at room temperature in the argon atmosphere until evolution of hydrogen had ceased. Then the allyl bromide (3.45 mmol) was dropped into the mixture and the stirring was continued for 1 h. The mixture was poured into water and extracted with diethyl ether. The organic layer was washed with brine and dried over $MgSO_4$. Then the solvent was removed, and the residue was purified by chromatography on silica gel to produce **13b**, **13c**, **14**, or **23**.

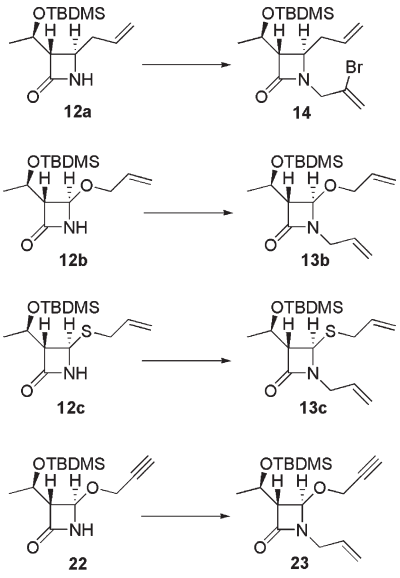

*(3R,4R)-1-But-3-enyl-3-[(1R)-(tert-butyl-dimethyl-silanyloxy)-ethyl]-4-vinyloxy-azetidin-2-one (**13b**).* Chromatographed using 10% AcOEt in hexane, colorless oil, yield 87%. $[\alpha]_D$ 12.0 (*c* 0.56, CH_2Cl_2). IR (film) ν/cm^{-1}: 1769, 1092, 837, 778. ^1H NMR (500 MHz, $CDCl_3$) δ/ppm: 0.05 (s, 3H), 0.08 (s,3H), 0.87 (s, 9H), 1.25 (d, *J* = 6.3 Hz, 3H), 2.99 (d, *J* = 3.8 Hz, 1H), 3.72 (ddt, *J* = 15.7, 6.8, 1.2 Hz, 1H), 3.95 (ddt, *J* = 15.7, 5.4, 1.6 Hz, 1H), 4.04−4.11 (m, 2H), 4.14−4.18 (m, 1H), 5.04 (bd, *J* = 1.2 Hz, 1H), 5.18−5.22 (m, 2H), 5.25−5.33 (m, 2H), 5.75−5.83 (m, 1H), 5.86−5.94 (m, 1H). ^{13}C NMR (125 MHz, $CDCl_3$) δ/ppm: −4.9, −4.6, 17.9, 22.6, 25.7(3C), 43.0, 64.2, 64.6, 68.8, 83.3, 117.1, 118.2, 132.2, 133.9, 166.8. Elemental Analysis calcd for $C_{17}H_{31}NO_3Si$: C, 62.73; H, 9.60; N, 4.30. Found: C, 62.78; H, 9.55; N, 4.35. HR MS (LSI) calcd for $[M + Na]^+$ $C_{17}H_{31}NO_3NaSi$ 348.1965, found 348.1978.

*(3S,4R)-1-But-3-enyl-3-[(1R)-(tert-butyl-dimethyl-silanyloxy)-ethyl]-4-vinylsulfanyl-azetidin-2-one (**13c**).* Chromatographed using 5% AcOEt in hexane, colorless oil, yield 82%. $[\alpha]_D$ 52.9 (*c* 0.50, CH_2Cl_2). IR (film) ν/cm^{-1}: 1763, 1722, 1251, 1146, 1136, 1061, 962, 836, 778. ^1H NMR (500 MHz, $CDCl_3$) δ/ppm: 0.07 (s, 3H), 0.09 (s, 3H), 0.89 (s, 9H), 1.23 (d, *J* = 6.3 Hz, 3H), 3.16 (t, *J* = 2.3 Hz, 1H), 3.22 (d, *J* = 7.6 Hz, 2H), 3.60 (ddd, *J* = 15.8, 7.0, 0.8 Hz, 1H), 4.06 (ddt, *J* = 15.8, 5.0, 1.5 Hz, 1H), 4.27 (qd, *J* = 6.3, 3.1 Hz, 1H), 4.80 (d, *J* = 2.2 Hz, 1H), 5.13−5.24 (m, 2H), 5.30 (dd, *J* = 17.1, 1.2 Hz, 1H), 5.76−5.89 (m, 2H). ^{13}C NMR (125 MHz, $CDCl_3$) δ/ppm: −4.8, −4.6, 17.9, 22.3, 25.7(3C), 33.1, 42.4, 57.6, 64.5, 65.0, 117.8, 118.4, 132.1, 134.1, 166.4. HR MS (ESI) calcd for $[M + Na]^+$ $C_{17}H_{31}NO_3NaSiS$ 364.1737, found 364.1729.

*(3S,4R)-4-Allyl-1-(2-bromo-allyl)-3-[(1R)-(tert-butyl-dimethyl-silanyloxy)-ethyl]-azetidin-2-one (**14**).* Chromatographed using 5% AcOEt in hexane, colorless oil, yield 47%. $[\alpha]_D$ −12.4 (*c* 0.66, CH_2Cl_2). IR (film) ν/cm^{-1}: 1760. ^1H NMR (500 MHz, $CDCl_3$) δ/ppm: 0.06 (s, 3H), 0.08 (s, 3H), 0.88 (s, 9H), 1.22 (d, *J* = 6.2 Hz, 3H), 2.39−2.34 (m, 1H), 2.53−2.49 (m, 1H), 2.84 (dd, *J* = 5.7, 2.1 Hz, 1H), 3.77 (m, 1H), 3.85 (d, *J* = 16.3 Hz, 1H), 4.18 (p, *J* = 6.1 Hz, 1H), 4.24 (d, *J* = 16.3 Hz, 1H), 5.18−5.11 (m, 2H), 5.60 (m, 1H), 5.82−5.74 (m, 1H), 5.86 (m, 1H). ^{13}C NMR (125 MHz, $CDCl_3$) δ/ppm: −4.3, −4.1, 18.3, 23.3, 26.2, 37.48, 48.9, 54.9, 63.4, 66.2, 118.7, 119.6,

127.9, 133.6, 168.0. HR MS (LSI) calcd for $[M + Na]^+$ $C_{17}H_{30}NO_2NaSiBr$ 410.1121, found 410.1118.

*(3R,4R)-1-Allyl-3-[(1R)-(tert-butyl-dimethyl-silanyloxy)-ethyl]-4-prop-2-ynyloxy-azetidin-2-one (**23**).* Chromatographed using 15% AcOEt in hexane, colorless oil, yield 93%. $[\alpha]_D$ 9.1 (*c* 0.87, CH_2Cl_2). IR (film) ν/cm^{-1}: 1767, 1645, 1472, 1258. ^1H NMR (500 MHz, $CDCl_3$) δ/ppm: 0.06 (s, 3H), 0.08 (s, 3H), 0.88 (s, 9H), 1.27 (d, *J* = 6.3 Hz, 3H), 2.48 (t, *J* = 2.4 Hz, 1H), 3.05 (dd, *J* = 3.8, 1.2 Hz, 1H), 3.74 (ddd, *J* = 15.7, 6.8, 1.1 Hz, 1H), 3.95 (ddt, *J* = 15.7, 5.5, 1.5 Hz, 1H), 4.17 (dq, *J* = 6.3, 3.8 Hz, 1H), 4.22 (dd, *J* = 2.6, 0.5 Hz, 2H), 5.18 (d, *J* = 1.0 Hz, 1H), 5.21 (dq, *J* = 10.2, 1.0 Hz, 1H), 5.29 (dq, *J* = 17.1, 1.4 Hz, 1H), 5.80 (dddd, *J* = 17.1, 10.2, 6.8, 5.5 Hz, 1H). ^{13}C NMR (125 MHz, $CDCl_3$) δ/ppm: −4.8, −4.5, 17.90, 22.6, 25.8(3C), 40.2, 55.5, 64.2, 64.7, 75.1, 79.2, 83.2, 118.5, 132.1, 166.6. HR MS (ESI) calcd for $[M + Na]^+$ $C_{17}H_{29}NO_3NaSi$ 346.1809, found 346.1822.

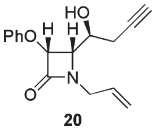

20

*(3R,4S)-1-Allyl-4-[(1S)-hydroxy-but-3-ynyl)]-3-phenoxy-azetidin-2-one (**20**).* A mixture of compound **15** (1 g, 4.3 mmol), zinc powder (1.7 g, 26.0 mmol), THF (10 mL), and saturated solution of ammonium chloride (25 mL) was cooled to −15 °C. Then propargyl bromide was added (1.4 mL, 13.0 mmol), and the mixture was stirred at −15 °C for 4 h. Then the insoluble material was filtered off and washed with THF. The filtrate was washed with ethyl acetate and dried over $MgSO_4$. Then the solvent was evaporated, and the residue was purified by chromatography on silica gel (15% AcOEt in hexane) to produce **16** (860 mg, 73%) as colorless oil. $[\alpha]_D$ 149.6 (*c* 0.71, CH_2Cl_2). IR (film) ν/cm^{-1}: 1753, 1644, 1598, 1495, 1238. ^1H NMR (500 MHz, $CDCl_3$) δ/ppm: 2.04 (t, *J* = 2.7 Hz, 1H), 2.11 (s, 1H), 2.67 (ddd, *J* = 17.6, 4.6, 2.7 Hz, 1H), 2.78 (ddd, *J* = 17.6, 5.3, 2.7 Hz, 1H), 3.78 (ddt, *J* = 15.8, 6.3, 1.2 Hz, 1H), 4.11 (ddt, *J* = 15.8, 5.3, 1.4 Hz, 1H), 4.36 (dd, *J* = 7.8, 5.1 Hz, 1H), 5.24−5.29 (m, 1H), 5.30 (d, *J* = 5.1 Hz, 1H), 5.78−5.85 (m, 1H), 7.01−7.05 (m, 1H), 7.08−7.11 (m, 2H), 7.28−7.32 (m, 2H). ^{13}C NMR (125 MHz, $CDCl_3$) δ/ppm: 24.3, 44.6, 59.6, 69.3, 71.7, 79.4, 80.4, 115.9(2C), 118.9, 122.8, 129.7(2C), 131.8, 157.3, 165.9. HR MS (ESI) calcd for $[M + Na]^+$ $C_{16}H_{17}NO_3Na$ 294.1100, found 294.1091.

Acetylation of Alcohols 16 and 20. A solution of lactams **16** or **20** (0.73 mmol) in pyridine (6 mL) and acetic anhydride (3 mL) was kept at room temperature for 15 h. Then the reaction mixture was poured into water and extracted with diethyl ether. The organic layer was washed consecutively with 10% HCl and saturated solution of $NaHCO_3$ and dried over $MgSO_4$. Then the solvent was removed, and the residue was chromatographed on silica gel (5% AcOEt in hexane) to produce **17** or **21**.

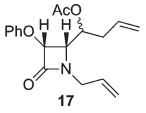

17

*Acetic Acid (2S,3R)-1-(1-Allyl-4-oxo-3-phenoxy-azetidin-2-yl)-but-3-enyl Ester (**17**).* Colorless oil, yield 90%. IR (film) ν/cm^{-1}: 1765, 1643, 1598, 1495, 1231. ^1H NMR (500 MHz, $CDCl_3$) δ/ppm: 1.93 (s, 3H), 2.05 (s, 3.6H), 2.34−2.44 (m, 2.2H), 2.55 (ddt, *J* = 6.3, 4.9, 1.4 Hz, 1.2H), 2.58 (ddt, *J* = 6.3, 4.9, 3.3 Hz, 1H), 3.63−3.68 (m, 1.2H), 3.69−3.73 (m, 1H), 4.05 (dd, *J* = 7.3, 5.3 Hz, 1.2H), 4.10 (dd, *J* = 5.2, 4.1 Hz, 1H), 4.16 (ddt, *J* = 15.8, 5.3, 1.6 Hz, 1.2H), 4.24 (ddt, *J* = 15.4, 5.2, 1.6 Hz, 1H), 5.06−5.11 (m, 2.2H), 5.23−5.29 (m, 8.8H), 5.36−5.40 (m, 2.2H), 5.71−5.82 (m, 4.4H), 7.00−7.06 (m, 2.2H), 7.07−7.10 (m, 4.4H), 7.28−7.34 (m, 4.4H). **Data for 17a**: ^{13}C NMR (125 MHz, $CDCl_3$) δ/ppm: 21.00, 36.56, 44.26, 59.05, 71.26, 79.99, 115.54(2C), 118.64, 122.47, 129.64(2C), 131.12, 133.06, 157.05, 166.12, 170.11. **Data for 17b**: ^{13}C NMR (125 MHz, $CDCl_3$) δ/ppm: 21.2, 35.2, 44.3, 58.3, 72.0, 80.0, 115.8(2C), 118.7, 129.6(2C), 131.4, 132.5, 157.5, 122.4, 166.2, 169.8. HR MS (ESI) calcd for $[M + Na]^+$ $C_{18}H_{21}NO_4Na$ 338.1263, found 338.1351.

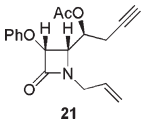

21

*Acetic Acid (1S)-1-[(2S,3R)-(1-Allyl-4-oxo-3-phenoxy-azetidin-2-yl)-but-3-ynyl Ester (**21**).* Colorless oil, yield 95%. $[\alpha]_D$ 91.7 (*c* 1.06, CH_2Cl_2). IR (film) ν/cm^{-1}: 3291, 1762, 1495, 1230, 1043, 756, 691. ^1H NMR (500 MHz, $CDCl_3$) δ/ppm: 2.04 (t, *J* = 2.7 Hz, 1H), 2.10 (s, 3H), 2.67 (ddd, *J* = 17.6, 4.6, 2.7 Hz, 1H), 2.78 (ddd, *J* = 17.6, 5.3, 2.7 Hz, 1H), 3.79 (ddt, *J* = 15.8, 6.3, 1.2 Hz, 1H), 4.11 (ddt, *J* = 15.8, 5.3, 1.4 Hz, 1H), 4.36 (dd, *J* = 7.8, 5.1 Hz, 1H), 5.30 (d, *J* = 5.1 Hz, 1H), 5.78−5.85 (m, 1H), 7.01−7.05 (m, 1H), 7.08−7.11 (m, 2H), 7.28−7.32 (m, 2H). ^{13}C NMR (125 MHz, $CDCl_3$) δ/ppm: 21.3, 21.5, 44.4, 57.6, 70.7, 71.5, 78.3, 80.1, 115.8(2C), 118.6, 122.6, 129.7(2C), 131.3, 157.4, 165.9, 169.7. HR MS (ESI) calcd for $[M + Na]^+$ $C_{16}H_{17}NO_4Na$ 310.1049, found 310.1037.

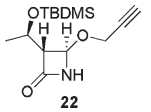

22

*(3R,4R)-3-[(1R)-(tert-Butyl-dimethyl-silanyloxy)-ethyl]-4-prop-2-ynyloxy-azetidin-2-one (**22**).* A mixture of acetoxyazetidinone **11** (2 g, 6.96 mmol), powdered $Zn(OAc)_2 \cdot 2H_2O$ (0.92 g, 4.18 mmol), toluene (25 mL), and propargyl alcohol (1.34 mL, 22.97 mmol) was refluxed for 6 h. Then the insoluble material was filtered off and washed with THF. Then the solvent was evaporated from the filtrate, and the residue was purified by chromatography on silica gel (15% AcOEt in hexane) to produce **22** (1.36 g, 69%) as colorless oil. $[\alpha]_D$ −19.3 (*c* 0.94, CH_2Cl_2). IR (film) ν/cm^{-1}: 1767, 1726, 1472, 1256. ^1H NMR (500 MHz, $CDCl_3$) δ/ppm: 0.07 (s, 3H), 0.08 (s, 3H), 0.88 (s, 9H), 1.27 (d, *J* = 6.3 Hz, 3H), 2.49 (t, *J* = 2.4 Hz, 1H), 3.09 (dd, *J* = 4.0, 1.2 Hz, 1H), 4.17 (dq, *J* = 6.3, 4.0 Hz, 1H), 4.24 (dd, *J* = 8.2, 2.4 Hz, 2H), 5.24 (d, *J* = 1.0 Hz, 1H), 6.44 (bs, 1H). ^{13}C NMR (125 MHz, $CDCl_3$) δ/ppm: −5.1, −4.3, 17.9, 22.4, 25.7(3C), 55.8, 64.2, 66.0, 75.3, 79.1, 80.3, 167.2. HR MS (ESI) calcd for $[M + Na]^+$ $C_{14}H_{25}NO_3NaSi$ 306.1496, found 306.1495. Elemental Analysis calcd for $C_{14}H_{25}NO_3Si$: C, 59.32; H, 8.89; N, 4.94. Found: C, 59.25; H, 8.86; N, 4.94.

■ ASSOCIATED CONTENT

Supporting Information. ^1H and ^{13}C NMR spectra of all new compounds, crystallographic data (CIF) of compound **1b**, information about details of calculated UV and CD spectra, total energies, relative energies, and Cartesian coordinates for all optimized structures used in this work. This material is available free of charge via the Internet at http://pubs.acs.org.

AUTHOR INFORMATION

Corresponding Author

*E-mail: jadwiga.frelek@icho.edu.pl; filipp.furche@uci.edu; grimmes@uni-muenster.de.

ACKNOWLEDGMENT

This work was supported by the Ministry of Science and Higher Education, grant nos. N N204 123537 (M.W.) and N N204 092935(J.F., A.B., K.M.), and by the DFG in the framework of the International Research Training Group 1444 with a scholarship to H.K. F.F. acknowledges support by the Center for Chemical Innovation "Chemistry at the Space-Time Limit" (CaSTL) of the NSF, grant no. CHE-0802913.

REFERENCES

(1) (a) Mann, J.; Crabbe, M. J. C. *Bacteria and Antibacterial Agents*; Oxford University Press: New York, 1996. (b) Cooper, R. D. G. *Topics in Antibiotics Chemistry*; Ellis Horwood Ltd.: Chichester, 1980. (c) Brown, A. G.; Butterworth, D.; Cole, M.; Hanscomb, G.; Hood, J. D.; Reading, C.; Rolinson, G. N. *J. Antibiot.* **1976**, *29*, 668–669.

(2) Sweet, R. M.; Dahl, L. I. *J. Am. Chem. Soc.* **1970**, *92*, 5489–5507.

(3) (a) Boyd, D. B. *J. Am. Chem. Soc.* **1972**, *94*, 6513–6519. (b) Toome, V.; Wegrzynski, B.; Reymond, G. *Biochem. Biophys. Res. Commun.* **1976**, *69*, 206–211. (c) Busson, R.; Roets, E.; Vanderhaeghe, H. *J. Org. Chem.* **1978**, *43*, 4438–4441.

(4) (a) Boyd, D. B. *J. Med. Chem.* **1973**, *16*, 1195–1199. (b) Rehling, H.; Jensen, H. *Tetrahedron Lett.* **1972**, *27*, 2793–2796. (c) Ogura, H.; Takayanagi, H.; Kubo, K.; Furuhata, K. *J. Am. Chem. Soc.* **1973**, *95*, 8056–8059. (d) Ogura, H.; Takeda, K.; Takahashi, H. *Chem. Pharm. Bull.* **1975**, *23*, 2469–2473. (e) McCann, J.; Rauk, A.; Shustov, G. V.; Wieser, H.; Yang, D. *Appl. Spectrosc.* **1996**, *50*, 630–641. (f) Galle, D.; Tolksdorf, M.; Braun, M. *Tetrahedron Lett.* **1995**, *36*, 4217–4720. (g) Wolf, H. *Tetrahedron Lett.* **1966**, 5151–5156. (h) Barbaro, G.; Battaglia, A.; Guerrini, A.; Bertucci, C.; Geremia, S. *Tetrahedron: Asymmetry* **1998**, *9*, 3401–3409. (i) Polonski, T.; Milewska, M. J. *Croat. Chim. Acta* **1989**, *62*, 129–134.

(5) Łysek, R.; Borsuk, K.; Chmielewski, M.; Kałuża, Z.; Urbańczyk-Lipkowska, Z.; Klimek, A.; Frelek, J. *J. Org. Chem.* **2002**, *67*, 1472–1479.

(6) (a) Cierpucha, M.; Solecka, J.; Frelek, J.; Szczukiewicz, P.; Chmielewski, M. *Biorg. Med. Chem.* **2004**, *12*, 405–416. (b) Frelek, J.; Łysek, R.; Borsuk, K.; Jagodziński, J.; Furman, B.; Klimek, A.; Chmielewski, M. *Enantiomer* **2002**, *7*, 107–114. (c) Chmielewski, M.; Cierpucha, M.; Kowalska, P.; Kwit, M.; Frelek, J. *Chirality* **2008**, *20*, 621–627.

(7) Frelek, J.; Kowalska, P.; Masnyk, M.; Kazimierski, A.; Korda, A.; Woźnica, M.; Chmielewski, M.; Furche, F. *Chem.—Eur. J.* **2007**, *13*, 6732–6744.

(8) Woźnica, M.; Kowalska, P.; Łysek, R.; Masnyk, M.; Górecki, M.; Kwit, M.; Furche, F.; Frelek, J. *Curr. Org. Chem.* **2010**, *14*, 1022–1036.

(9) Woźnica, M.; Masnyk, M.; Stecko, S.; Mames, A.; Furman, B.; Chmielewski, M.; Frelek, J. *J. Org. Chem.* **2010**, *75*, 7219–7226.

(10) Elliot, P.; Furche, F.; Burke, K. *Rev. Comp. Chem.* **2009**, *26*, 91–165.

(11) (a) Vintonyak, V. V.; Warburg, K.; Kruse, H.; Grimme, S.; Hubel, K.; Rauh, D.; Waldmann, H. *Angew. Chem., Int. Ed.* **2010**, *49*, 5902–5905. (b) Goerigk, L.; Grimme, S. *J. Phys. Chem. A* **2009**, *113*, 767–776. (c) Mori, T.; Grimme, S.; Inoue, Y. *J. Org. Chem.* **2007**, *72*, 6998–7010. (d) Bringmann, G.; Bruhn, T.; Maksimenka, K.; Hemberger, Y. *Eur. J. Org. Chem.* **2009**, 2717–2727. (e) Stephens, P. J.; Pan, J. J.; Devlin, F. J.; Urbanova, M.; Julinek, O.; Hajicek, J. *Chirality* **2008**, *20*, 454–470. (f) Stephens, P. J.; Pan, J. J.; Devlin, F. J.; Urbanova, M.; Hajicek, J. *J. Org. Chem.* **2007**, *72*, 2508–2524.

(12) Alcaide, B.; Sierra, M.; Polanco, C. *J. Org. Chem.* **1998**, *63*, 6786–6796.

(13) Kang, S.; Baik, T.; Jiao, X.; Lee, K.; Lee, C. *Synlett* **1999**, *4*, 447–449.

(14) (a) Pedersen, B. S.; Scheibye, S.; Nilsson, N. H.; Lawesson, S.-O. *Bull. Soc. Chim. Belg.* **1978**, *87*, 223–228. (b) Scheibye, S.; Kristensen, J.; Lawesson, S.-O. *Tetrahedron* **1978**, *35*, 1339–1343.

(15) *PCModel 9.1*; Serena Software: Bloomington, 2005.

(16) Grimme, S. *J. Comput. Chem.* **2006**, *27*, 1787–1799.

(17) (a) Lee, C. T.; Yang, W. T.; Parr, R. G. *Phys. Rev. B* **1988**, *37*, 785–789. (b) Becke, A. D. *Phys. Rev. A* **1988**, *38*, 3098–3100.

(18) Weigend, F.; Ahlrichs, R. *Phys. Chem. Chem. Phys.* **2005**, *7*, 3297–3305.

(19) Grimme, S. *J. Chem. Phys.* **2006**, *124*, 034108.

(20) Ahlrichs, R.; Armbruster, M. K.; Bär, M., Baron, H.-P.; Bauernschmitt, R.; Crawford, N.; Deglman, P.; Ehrig, M.; Eichkorn, K.; Elliott, S.; Furche, F.; Haase, F.; Häster, M.; Hättig, C.; Hellweg, H.; Horn, H.; Huber, C.; Huniar, U.; Kattannek, M.; Kömel, C.; Kollwitz, M.; May, P.; Nava, P.; Ochsenfeld, C.; Öhm, H.; Patzelt, D.; Rappoport, D.; Rubner, O.; Schäfer, A.; Schneider, U.; Sierka, M.; Treutler, O.; Unterreiner, B.; von Arnim, M.; Weigand, F.; Weis, P.; Weiss, H. *TURBOMOLE Vers. 6.0*; University of Karlsruhe: Karlsruhe, 2009. See also: www.turbomole.com.

(21) Vahtras, O.; Almlof, J.; Feyereisen, M. W. *Chem. Phys. Lett.* **1993**, *213*, 514–518.

(22) Feyereisen, M.; Fitzgerald, G.; Komornicki, A. *Chem. Phys. Lett.* **1993**, 359–363.

(23) Hattig, C.; Weigend, F. *J. Chem. Phys.* **2000**, *113*, 5154–5161.

(24) Furche, F.; Rappoport, D. In *Density Functional Methods for Excited States:Equilibrium Structure and Electronic Spectra*; Elsevier: Amsterdam, 2005.

(25) (a) Treutler, O.; Ahlrichs, R. *J. Chem. Phys.* **1995**, *102*, 346–354. (b) Eichkorn, K.; Weigend, F.; Treutler, O.; Ahlrichs, R. *Theor. Chem. Acc.* **1997**, *97*, 119–124.

(26) Perdew, J. P.; Ernzerhof, M.; Burke, K. *J. Chem. Phys.* **1996**, *105*, 9982–9985.

(27) Radhakrishnan, T. P.; Agranat, I. *Struct. Chem.* **1991**, *2*, 107–115.

(28) (a) Yde, B.; Yousif, N. M.; Pedersen, U.; Thomsen, I.; Lawesson, S.-O. *Tetrahedron* **1984**, *40*, 2047–2052. (b) Maciejewski, A.; Steer, R. P. *Chem. Rev.* **1993**, *93*, 67–98.

(29) Kajtar, M.; Kajtar, J.; Maier, Z.; Zewdu, M.; Hollosi, M. *Spectrochim. Acta* **1993**, *48B*, 87–91.

(30) Penfold, D. J.; Pike, K.; Genge, A.; Anson, M.; Kitteringham, J.; Kilburn, J. D. *Tetrahedron Lett.* **2000**, *41*, 10347–10351.

(31) Perrin, D. D.; Armarego, W. L. F.; Perrin, D. R. *Purifications of Laboratory Chemicals*; Pergamon Press: Oxford, 1980.